1977

Wave Energy and Beach Response for Three Southern Rhode Island Beaches

Nancy Susan Donovan
University of Rhode Island

WAVE ENERGY AND BEACH RESPONSE FOR THREE SOUTHERN RHODE ISLAND BEACHES

BY

NANCY SUSAN DONOVAN

A THESIS SUBMITTED IN PARTIAL FULFILLMENT OF THE REQUIREMENTS FOR THE DEGREE OF

MASTER OF SCIENCE

IN

OCEANOGRAPHY

UNIVERSITY OF RHODE ISLAND

1977

ABSTRACT

Wave characteristics, longshore drift velocities and beach elevation changes were monitored at Weekapaug, East, and Green Hill beaches on southwestern Rhode Island's moderate energy shoreline. Results showed that erosion was generally the consequence of southeast waves while accretion was usually associated with southwest waves. Also, measured longshore velocities were fastest at Green Hill, slower at Weekapaug and slowest at East Beach. Stronger littoral currents at Weekapaug and Green Hill beaches probably resulted from the closer proximity of potentially steeper longshore hydraulic gradients associated with adjacent headlands.

As no field observations were available regarding nearshore circulation, the longshore component of wave power curves and generated breaker heights from a mathematical model (May and Tanner, 1973) were used to suggest circulation patterns. For oblique wave approaches, both sets of data indicated that small circulation cells tended to stack on the windward sides of headlands with longer cells to leeward.

Field data were compared with the computer model output for three cases of beach erosion-deposition response. In each case the model provided the correct simple response but did not indicate a compound response of erosion on the foreshore and deposition on the backshore. Furthermore the model failed to successfully predict the representative field example for non-uniform response; i.e., erosion at Weekapaug and Green Hill and deposition at East. However the theory related to the model was used to demonstrate that refraction in a beach re-entrant is responsible not only for the magnitude of the cutting and filling response but also for the uniform and non-uniform erosional and

accretional responses.

An evaluation of the model revealed that initial grid size and ray spacing were responsible for the predicted longshore energy distribution and drift direction. Moreover rapid bathymetric changes, shoals, and surf zones caused the model to breakdown due to mathematical limitations. Further longshore speed forecasts were greater than measured because the model was incapable of considering reformed smaller waves. Finally no positive correlation between storm and fair-weather seasonal ΔP_L curves and their corresponding seasonal elevation changes were found because a sufficient wave spectrum was not available to be considered.

ACKNOWLEDGEMENT

I wish to thank those people who so generously provided their time, expertise, and equipment during this study.

Drs. H. E. Winn, F. H. Middleton, L. R. Leblanc, and T. A. Napora gave equipment and advice. Dr. C. A. Oviatt supplied data. I am also indebted to G. Rogers and G. Urban in Maintenance for providing equipment, J. Allan and his jeep for his assistance, M. Leonard for drafting the figures and S. Proulx for typing the thesis.

Special thanks are due to Drs. J. A. Knauss, C. A. Griscom, J. C. Boothroyd, and P. C. Cornillon for reading the thesis and their suggestions during the study. An extra-special thanks is due to Dr. R. L. McMaster for his guidance during the study and his incredible patience during the writing of the thesis.

I am also grateful to Douglas for his continued support through all of the study.

PREFACE

The Thesis is written in Manuscript form in anticipation of future publication. Detailed discussion of the methods, breaker energy, wave attenuation, influence of period and height on longshore power, and volume calculation are in the appendices.

TABLE OF CONTENTS

LIST OF TABLES

LIST OF ILLUSTRATIONS

I. INTRODUCTION

Location

The southwestern Rhode Island coast, trending east-northeast-west-southwest, is 30 km long from Point Judith to Watch Hill Point, and consists of a series of headlands and interconnecting barrier splits with salt ponds lying behind the splits (Fig. 1). This coast faces Block Island Sound, the most seaward part of the Long Island-Block Island Sound system. The sound is effectively sheltered on its southern limit by Long Island and Block Island, but is more exposed toward the southeastern, eastern, and east-northeastern directions.

Previous Studies

Following the disastrous 1938 hurricane, several studies concerning beach erosion and beach processes were undertaken along Rhode Island's southwestern coastline. Nichols and Marston (1939) described the dune destruction and the appearance of new inlets scoured through the beaches by the 1938 hurricane waves and tides. Subsequently, the Corps of Engineers (1950) assessed and catalogued the effects of storms on these beaches. The investigation showed storms with winds from the south and southeast are infrequent, but are more severe. To demonstrate this finding, a compilation of offshore wave directions indicated a distinct prominence of easterly swells 2m and greater. The report also described a rudimentary littoral drift pattern for this stretch of beaches.

More recent studies of beach processes include those conducted by

Figure 1. Map of southwestern Rhode Island shore with the underwater topography of adjacent Block Island Sound.

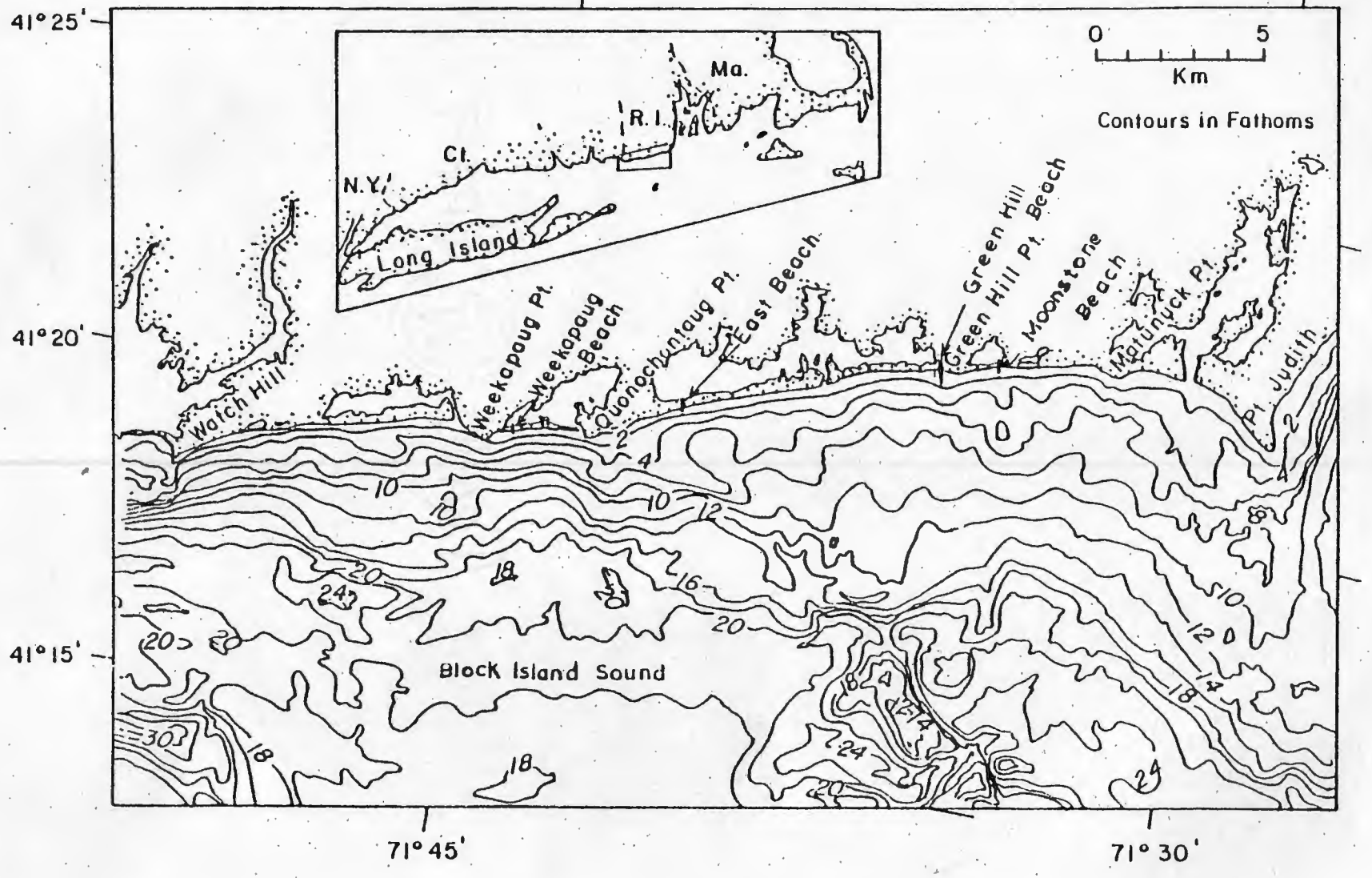
41°25'
41°20'
41°15'
71°45'
71°30'
0
5
Km
Contours in Fathoms
Ma.
R.I.
Ct.
N.Y.
Long Island
Watch Hill
Weekapaug Pt.
Weekapaug Beach
Quonochontaug Pt.
East Beach
Green Hill
Green Hill Pt.
Beach
Moonstone Beach
Matunuck Pt.
Pt. Judith
Block Island Sound

McMaster (1960) and Beale (1975). McMaster (1960) extended the understanding of beach drift from Watch Hill to Point Judith, based upon significant changes in heavy mineral composition of the foreshore beach sand. He found that the net beach drift converges westward toward Charlestown Inlet and diverges from a position near Matunuck Point, suggesting beach circulation cells for this stretch of shoreline. However, the energy agents responsible for these cells were not examined nor was consideration given to the changing nearshore circulation patterns under differing wave regimes. In the vicinity of Matunuck Point Beale (1975) extended McMaster's study by investigation of the movement of sand under wave and tide conditions in both the foreshore and nearshore zones. He found that beach circulation cells described by McMaster (1960) are present and are maintained by the refracted southeast swells.

In 1961 a biweekly transit survey was initiated to record periods of erosion and accretion over yearly cycles at Moonstone, Green Hill, East, and Weekapaug Beaches (McMaster, 1961) (Fig. 1). A comparison of profiles from this survey indicated these beaches may not erode and/or accrete in a uniform manner under a given set of wave characteristics. The study raised the questions as to what parameters cause the non-systematic behavior and why the response is so persistent.

A promising approach of furnishing answers to these kinds of questions was developed by May and Tanner (1973) for the west coast Florida beaches. They wrote a computer model to provide a method of predicting shoreline changes from the approximation of the longshore drift gradient. This program, given deep water wave characteristics, will generate the total power of a breaking wave and the longshore

power component of the wave. The gradient between the points of longshore drift, the littoral power gradient, is then determined graphically. This indicates where erosion, transportation, or deposition is taking place along a shoreline. The model's output was favorably tested against observations made on Florida's low energy beaches.

Hence, a 13 km mid-section of Rhode Island shoreline which included Weekapaug, East, and Green Hill Beach stations (Fig. 1) was selected for detailed studies of waves, nearshore circulation, and beach level changes by means of field observations between September 1974 and September 1975. These observations were compared with longshore drift speeds and beach erosional-depositional potential as produced by the May and Tanner computer model for the same shoreline segment. The purpose of this investigation was to (1) compare the two procedures used to infer the littoral circulation directions; (2) show why the observed longshore velocities have a distinct variation; (3) explain the uniform and non-uniform beach responses in the shoreline segment; and (4) evaluate the applicability of the May and Tanner (1973) model to the moderate energy Rhode Island coast.

II. GENERAL SETTING

Meteorology

Rhode Island's weather is influenced by the migration of the jet-stream, or circumpolar circulation, and the Bermuda High (Havens et al., 1972). In the fall, as the circumpolar circulation expands, the winds become stronger and more intense northeast storms pass through the region. In the spring circumpolar circulation contracts allowing the Bermuda High to expand (Havens et al., 1972). Under the influence of the Bermuda High the winds are gentle and from the southwest. During this season storms generally follow the coast as they move north.

Physical Oceanography

For this study the most important aspects of physical oceanography are the waves and tides. The predominant southerly and southeasterly waves impinging on the southern Rhode Island shore are due to the refraction by the offshore landforms (Fig. 1). These swells are generated by storms along the Atlantic coast, with the highest swells from the east (Corps of Engineers, 1950). Southwest waves are produced in Long Island and Block Island Sounds. In the winter and fall the overall wave climate is more severe (Anonymous, 1975), because of the prevailing weather patterns (Bumpus, 1972).

In Block Island Sound the tide is semi-diurnal and has a range of 1m (Anonymous, 1976). Nearshore the tide is east-west oscillatory, but becomes rotary beyond the 6m isobath (Anonymous, 1975). For the major part of the tidal cycle along the shore the flood current flows

westward and is strongest in this direction. For this tidal stage the maximum flow is about 25 cm/s at Green Hill and approximately 55 cm/s at Weekapaug (Anonymous, 1971). The eastward ebb current is less than 25 cm/s for the southern Rhode Island shore.

Geology

Pleistocene glaciation has controlled the surficial geology of eastern Block Island Sound and coastal southwestern Rhode Island. The floor of the sound, consisting of glacial outwash and ground moraine, has been modified by stream flow which in many cases followed partially filled pre-glacial valleys before the rise of sea level. Ground moraine deposits not only form the shoals off the present coast (e.g. Nebraska Shoal) but also transect the modern shoreline trend at Weekapaug, Quonochontaug and Green Hill. However, bedrock outcrops, too, are associated with the moraine at Quonochontaug and Weekapaug Points.

The present barrier splits in the study area developed between the prongs of ground moraine. Following the ice retreat from the region, these barriers did not begin to form until the sea reached a stand of -5m below today's level, approximately 3,500 years B.P. (Dillon, 1970). With further transgression of the sea, the beaches could have drowned, built-up and remained stationary, or migrated depending upon the available sand supply and the rate of rise of sea level. Dillon (1970) has shown that, although the sea level rise was slow during this interval, the beaches were forced to migrate because of a limited supply of sand. Moreover, only the glacial deposits, which were reworked as the sea transgressed, could have supplied the available volume of sand.

Description of Beaches

Weekapaug, East and Green Hill Beaches, lying from 5 to 8 km apart, are located in each of three elongated, asymmetrical, shallow, shoreline re-entrants (Fig. 1). These are: Weekapaug to Quonochontaug Points; Quonochontaug to Charlestown Breachway; and the Breachway to Green Hill Point. Although Weekapaug and East are situated almost equally between their adjacent bayheads, the former is nearer to its headland than the latter. However, of the three beaches, Green Hill lies closest to a headland.

The general characteristics of these observational beaches are similar with respect to overall width, slope and grain size, but differ in other respects. Measured horizontally from the base of the dunes to the low tide mark, the breadths of Weekapaug, East and Green Hill Beaches are 36 m, 45 m, and 45 m respectively. The general slope at all three beaches is approximately 3°, and the sand is medium-grained. At Weekapaug Beach, a consistent slope occurs from the low dunes to the low water line, infrequent cusps tend to have long wavelengths and low amplitudes, and scarps are very rare. East Beach, on the other hand, is backed by prominent dunes, reveals a very distinctive berm year-round, frequently contains cusps that are shorter and deeper than at Weekapaug, and shows scarps that are more prevalent due to the year-round berm. At Green Hill the highest dunes occur, the slope is constant from the base of the dunes to the low water line, cusps are low amplitude and variable in wavelength, and scarps are uncommon.

Offshore Topography

The offshore topography can be generally characterized as stretches of regular parallel contours broken by shoals (Fig. 1). To the west of Weekapaug Beach is an attached southeast trending headland shoal, while the bathymetry contiguous to the beach is regular. Similarly, the topography off East Beach is smooth, but small shoals exist further offshore. To the west a lobate shoal trends southeasterly from Quonochontaug Point. The bottom configuration off Green Hill consists of two flanking shoals. The shoal to the southwest of the beach is small, attached and lobate while the other, Nebraska Shoal, to the southeast is large, detached, hummocky, and ovate.

III. PROCEDURES AND METHODS

On the three observational beaches, elevation profiles were measured and incident waves were observed from September 1974 to September 1975. The profiles were determined before and after storms and periodically in fair weather periods by using a handleveling and slope chaining method (Kelly, 1960). For detailed description of methods see Appendix A. Previously established reference points of the bi-weekly McMaster (1961) survey were occupied for leveling. Also, the concurrent profiles from the McMaster (1961) survey provided additional leveling data. By boat a single nearshore echo sounding survey was made adjacent to each study beach in early September 1975 in a manner similar to that of Bascom (1964). Two parallel lines, roughly 15 m apart were run to approximately the 9 m contour.

The important wave parameters, height, period, and approach angle were determined by modifying methods suggested by Peirson et al. (1955). The breaker height was measured by comparing the breaker to a marked pole while standing at the water line. Timing the waves with a stop-watch just as they broke provided a measure of the period. Finally, the approach angle was determined by sighting perpendicular to the wave fronts with a Brunton compass. When the surf conditions permitted, wooden blocks were thrown into the water to estimate the direction and magnitude of the littoral drift (Bascom, 1964).

In the laboratory the level data were processed and compiled for comparison with the May and Tanner (1973) model computer program. A hindcasting method (Bretschneider, 1952) was used to generate additional wave information for the program. Another source of tide and wave data for the program was obtained from New England Electric's Charlestown

Power Plant Project (Anonymous, 1975). For a final comparison, air photos taken after the December 1, 1974 northeast storm, were traced for the wave patterns.

IV. MAY AND TANNER MODEL

The May and Tanner model (1973) is formulated to predict shoreline changes by the interaction of waves and coastline geometry. Based upon refraction in a half re-entrant shore, the energy from impinging waves is highest at the headland and smallest at the bayhead (Fig. 2). Also, the wave orthogonals are perpendicular to the shore at the headland and bayhead due to convergence and divergence, respectively.

Longshore sand transport in a bay is best described in terms of energy per unit distance along the beach per unit time, which in cgs units is $g \cdot cm^2/s^3 \cdot cm$ or $g \cdot cm/s^3$. Since energy per unit time ($(g \cdot cm^2/s^2)(1/s)$) is power, the rate of doing work can be expressed as power per unit distance on the beach ($(g \cdot cm^2/s^2)(1/s)(1/cm)$). The littoral component of power, P_L, can then be defined by the power per unit distance and the angle β, between the wave normal and the perpendicular to the depth contours. P_L has the same units as shown in the above dimensional analysis. From the following equation

$$P_L = 0.5\ P_b \sin(2\beta) \qquad (1)$$

where P_b = total wave power per unit distance along the shoreline and 0.5 = constant, it is obvious that P_L is a direct function of $\sin(2\beta)$. Thus, as $\sin(2\beta) \to 0$, $P_L \to 0$, and as $\sin(2\beta) \to 1$, $P_L \to 0.5P_b$. Therefore there are two points where $\sin(2\beta)$ and P_L are zero; i.e., at the headland (a) and the bayhead (e) (Fig. 2). At the midpoint (c) along the re-entrant, the $\sin(2\beta)$ and P_L are maximum.

From P_L the transport rate, q, or the quantity of sand which crosses a line perpendicular to the beach per unit time, can be

Figure 2. Half re-entrant of the May and Tanner (1973) model. The littoral drift is shown moving from the headland (a) to the bayhead (e). Also indicated is the energy distribution for the half re-entrant and the associated curves P_L (q and I_L) and dq/dx. (After May and Tanner, 1973).

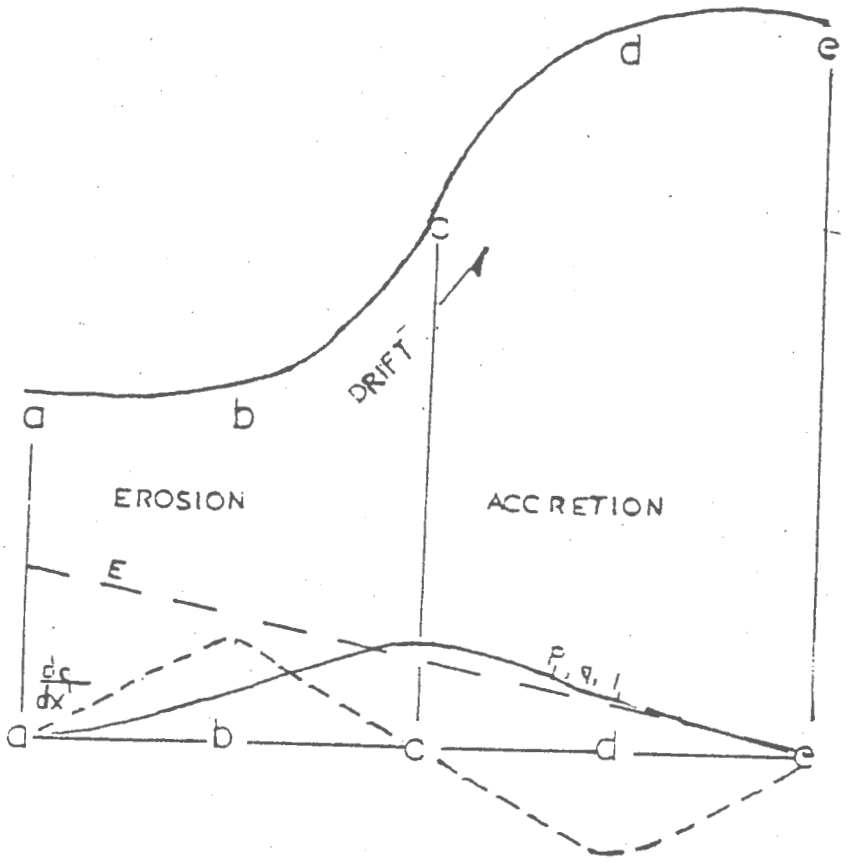
a
b
c
d
e
DRIFT
EROSION
ACCRETION
E
$\frac{dc}{dx}$
P, q, I

calculated. The empirical relation (Inman and Bagnold, 1963)

$$q = KP_L/\rho_s\gamma \qquad (2)$$

where ρ_s = mass density of the moving sand, γ = acceleration of gravity, and K = dimensionless numerical coefficient. Since q is a linear function of P_L, it has the same maximum and minimum points (Fig. 2). Going from a (P_L = 0) to c (P_L = maximum) on the q curve, the transport rate becomes larger for each successive increment and erosion is suggested. On the other hand following the q curve from c (P_L = maximum) to e (P_L = 0), the rate of transport values diminish for each increment and deposition is indicated. Another approach to understanding the importance of the transport rate is to examine the change in q per unit length of beach; i.e., dq/dx or equivalent ΔP_L. In the interval a to c, q increases rapidly per unit length initially (a to b) but then decelerates from b to c (Fig. 2). Thus, the intermediate point b is defined where erosion is at a maximum. Using the same method, a corresponding point maximizing deposition, d, is determined. Point c, where erosion and deposition are equal dq/dx = 0 (ΔP_L = 0) and is interpreted as being the position where transportation takes place. Thus for the change in delivery rate, dq/dx (ΔP_L), a, c, and e are zero and b and d are maxima for erosion and deposition, respectively. The positions of a, b, c, d, and e will vary with differing wave regimes, but they will all be present. Hence under a given wave regime the wave energy (E), the longshore power component (P_L) generated, and the transport rate (q) can all be related and used to describe the shoreline changes in a half re-entrant beach.

V. RESULTS

Field Observations

Wave Data

In general, waves approached Weekapaug, East and Green Hill Beaches from the southeast and southwest directions (Table 1), with the most frequent waves coming from the south-southeast at heights of 0.3 to 0.6 m and periods of 5 to 6 s (Table 1a). The southeast waves, propagated in the Atlantic, were 0.3 to 0.6 m high and had periods of about 8 s (Table 1). Those from the southwest were generated locally in Long Island and Block Island Sounds and were usually some 0.6 to 0.9 m in height with 5 to 6 s periods.

The most important event of the year was the December 1, 1974 northeast storm in which winds gusted to hurricane force. On the following day the decaying wave ensembles were coming from the southeast with average heights of 1.5 m and 12 s periods. Wave information from the Charlestown Hydrographic Study (Anonymous, 1975) agreed with the investigator's observations (Table 2).

Beach Profiles

Surveys were conducted at the three beaches simultaneously with wave observations. Weekapaug, a beach with constant slope and generally no berm (McMaster, 1961), responded in its usual manner by showing small vertical changes between the surveys. For example during a two week period, this beach revealed a 0.6 m elevational change (Fig. 3a). Interestingly after the passage of the severe December 1, 1974 northeast storm, the upper beach built-up while the lower foreshore showed no

Table 1. Wave Measurements

Date	Beach								
	Weekapaug			East			Green Hill		
	°T	T(s)	H(m)	°T	T(s)	H(m)	°T	T(s)	H(m)
9/ 5/74	140	7.0	0.61-0.92	135	9.0	0.15	135	8.0	0.15
9/12/74	180	4.0	0.30-0.61	180	4.0	0.30-0.61	180	4.0	0.30-0.61
9/26/74	200	4.5	0.15-0.30	125	8.5	0.30-0.61	160	7.0	0.30-0.61
10/11/74	160	5.0	0.15-0.30	160	5.0	0.15-0.30	142	5.5	0.15-0.30
10/24/74	130	7.5	0.30-0.61	135	8.0	0.61-0.92	138	7.5	0.61-0.92
11/ 4/74	128	9.0	0.30	132	7.0	0.61-0.92	160	12.0	0.30-0.61
11/12/74	130	6.0	0.61	120	6.0	0.61	150	6.0	0.61-1.22
11/14/74	190	6.0	0.61	194	6.0	0.61-0.92	196	6.0	0.92-1.22
12/10/74	140	12.0	0.92-1.53	150	12.0	0.92-1.53	Missing		
1/10/75	134	5.0	0.30-0.61	132	5.5	0.61-1.22	150	5.5	0.30-0.61
1/17/75	200	4.0	0.15-0.30	220	5.0	0.30-0.61	210	5.0	0.15-0.30
1/19/75	190	6.0	0.61-1.22	196	6.0	0.92-1.53	194	6.0	0.61-1.22
1/23/75	160	6.5	0.15-0.30	160	6.0	0.15-0.30	160	6.0	0.15-0.30
2/10/75	200	5.0	0.15-0.30	200	5.0	0.15-0.30	202	5.0	0.15-0.30
2/26/75	210	5.5	0.61-0.92	206	5.5	0.30-0.61	212	5.5	0.30-0.61
3/10/75	190	4.0	0.15-0.30	188	4.0	0.30-0.61	210	4.0	0.30-0.61
3/18/75	126	6.0	0.30-0.61	128	6.0	0.61-0.92	125	6.0	0.61-0.92
4/ 8/75	200	4.0	0.15-0.30	204	4.5	0.15-0.30	202	4.5	0.15-0.30
4/18/75	148	7.5	0.15-0.30	142	10.5	0.61-0.92	144	8.0	0.30-0.61
5/ 6/75	135	8.0	0.15-0.30	136	8.0	0.61-0.92	136	8.0	0.15-0.30
7/29/75	160	7.0	0.30-0.61	166	7.0	0.61-1.22	200	6.5	0.61-0.92
8/22/75	214	6.0	0.61-1.22	210	5.5	0.92-1.53	210	4.5	0.61-1.22
9/27/75	195	7.0	0.61-1.22	155	8.0	0.92-1.53	148	7.5	0.61-1.22

Table 1a. Ranges and Modes of Wave Data

Parameters	Ranges	Modes
Direction	SW-ESE	SSE
Height	0.1m-1.5m	0.3m-0.6m
Period	4s-12s	5s-6s

Table 2. Raytheon Wave Data

Time of Observation		Significant Wave Height (ft)									Maximum
Period	Duration (days)	<1.50	1.50-1.99	2.00-2.49	2.50-2.99	3.00-3.49	3.50-3.99	4.00-4.49	4.50-4.99	>5.00	Wave Height (ft)
Apr-June 1974 (Apr, 1975)	36	92.3	2.4	2.2	0.2	0.5	0.2	0.3	0.6	1.3	7.20
July-Sept 1974	90	73.2	11.9	10.4	2.3	0.7	0.9	0.3	0.2	0.1	5.39
Oct-Dec 1974*	30	46.7	26.1	10.1	5.6	1.5	1.0	0.7	1.1	7.2	6.74
Jan-Mar 1975	87	59.3	9.5	8.8	7.6	4.8	3.4	2.2	1.3	3.1	8.43
Cumulative	243	67.8	11.4	8.6	4.3	2.2	1.7	1.0	0.8	2.2	8.43

* Sensor moved from 32 ft below MLW to 19 ft MLW on November 19, 1974 (Raytheon Report, 1975).

Note that values in table under "Significant Wave Height" represent the percent frequency in each interval for a given period.

Figure 3. (a) The characteristic response of Weekapaug throughout the study. R_o is the permanent reference point for all surveys at this beach.

(b) The response of Weekapaug as a result of the December 1, 1974 northeast storm.

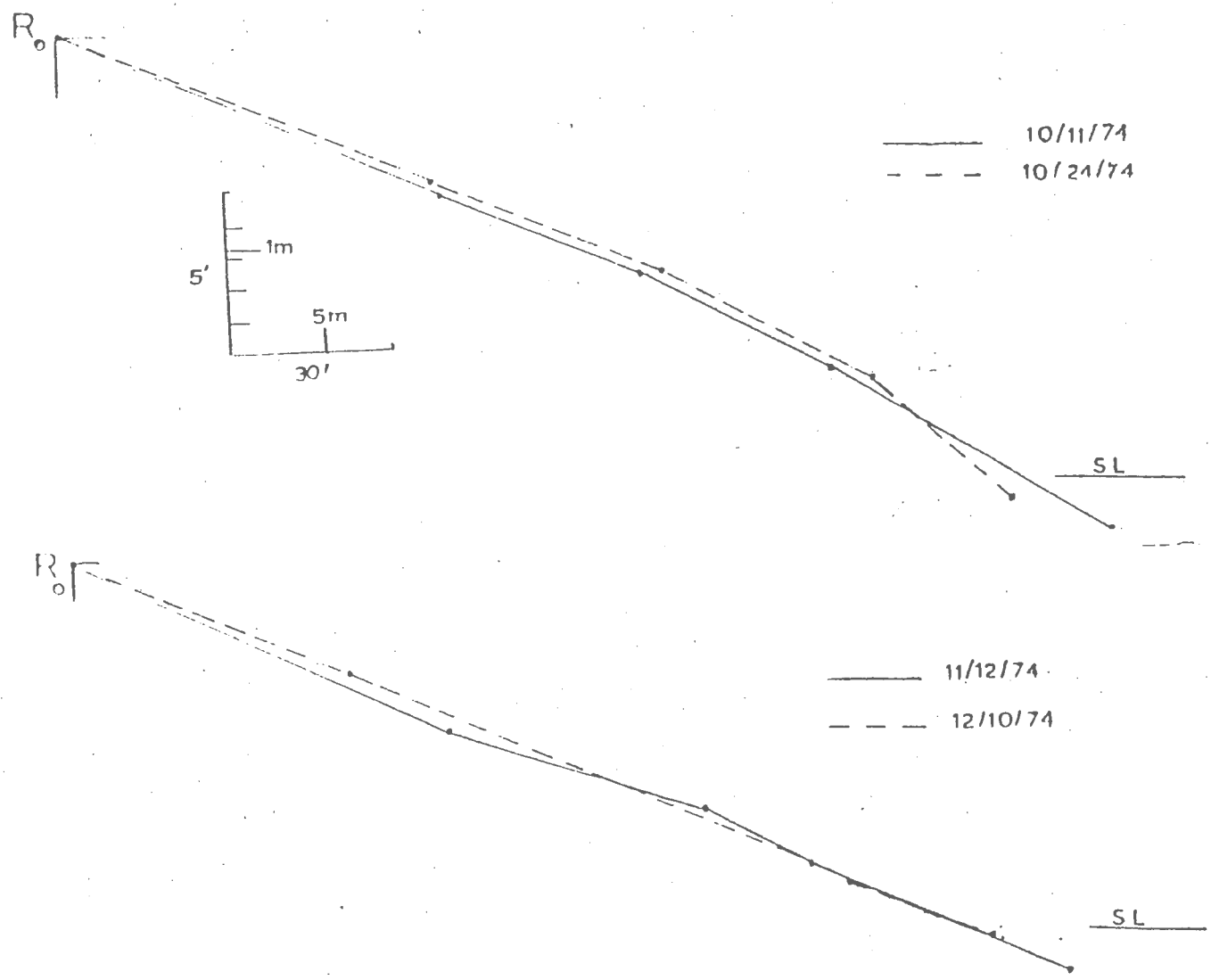
R_o
10/11/74
10/24/74
1m
5'
5m
30'
SL
R_o
11/12/74
12/10/74
SL

change or suffered only local erosion (Fig. 3b). However, for the year Weekapaug showed a general erosional response.

East Beach, with a predominate year-round berm on the foreshore, was identified as a beach that eroded and accreted large volumes of sand (McMaster, 1961). This response continued since it was not unusual for 1.1 m of erosion or accretion to occur on the foreshore (Fig. 4a). The December 1, 1974 storm caused 1.7 m of vertical erosion (Fig. 4b), which effectively removed the berm leaving the profile concave upward until March when the berm began to rebuild. As a first phase of erosion the berm frequently exhibited a scarp (Fig. 4a). For the year East Beach showed a net cutting response.

On Green Hill the amount of cutting and filling that occurred was more than that at Weekapaug, but less than that at East Beach (McMaster, 1961), and the response style remained the same. The beach showed a vertical change of generally no more than 0.6 m (Fig. 5a) and a net erosional response for the year. The December 1 northeast storm waves effectively cut into the dunes and spread the sand on the lower foreshore which produced an accretional condition on the beach face (Fig. 5b).

During this investigation the beaches did not always erode and/or accrete in unison which was documented previously (McMaster, 1961). The January and February surveys indicated East Beach had eroded 0.7 m on the foreshore and accreted 0.5 m on the backshore while Weekapaug and Green Hill accreted 0.3 m and 0.9 m, respectively (Fig. 6). Although East Beach's foreshore was cut-back and Green Hill and Weekapaug were built-out, the phenomenon of non-uniform response was not limited to this order; i.e., Green Hill could have eroded while Weekapaug and East Beach were prograding.

Figure 4. (a) Certain East Beach responses. Profiles from September 26 and October 11, 1974 show a scarp as a result of cutting. Also a large cutting response (1.1 m) is shown by profiles from September 12 and 26, 1974.

(b) The response of East Beach as a result of the December 1, 1974 northeast storm.

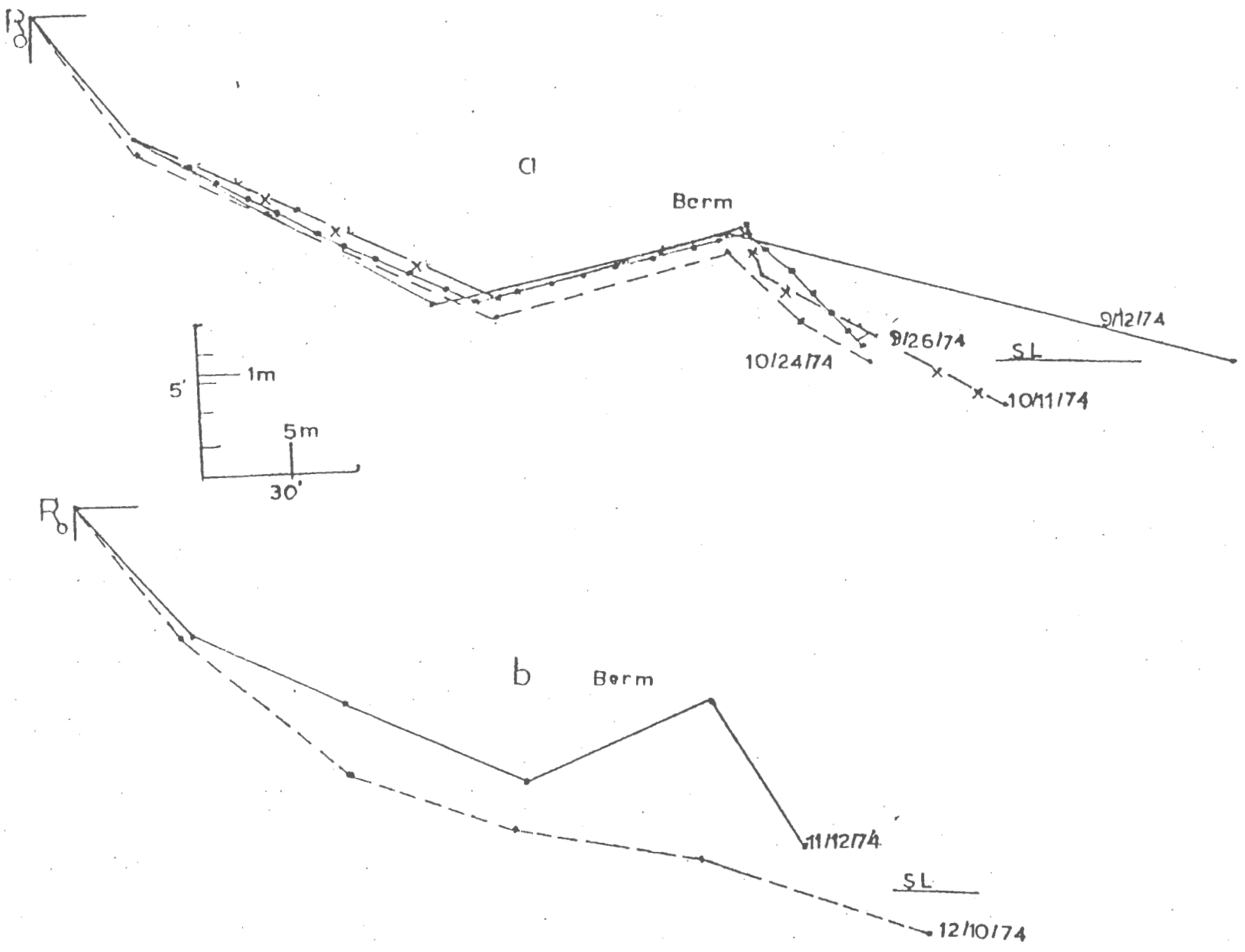
a
Berm
9/12/74
9/26/74
10/24/74
SL
10/11/74
5'
1m
5m
30'
b
Berm
11/12/74
SL
12/10/74

Figure 5. (a) The characteristic response of Green Hill during the study.

(b) The accretional response of Green Hill as a result of the December 1, 1974 northeast storm.

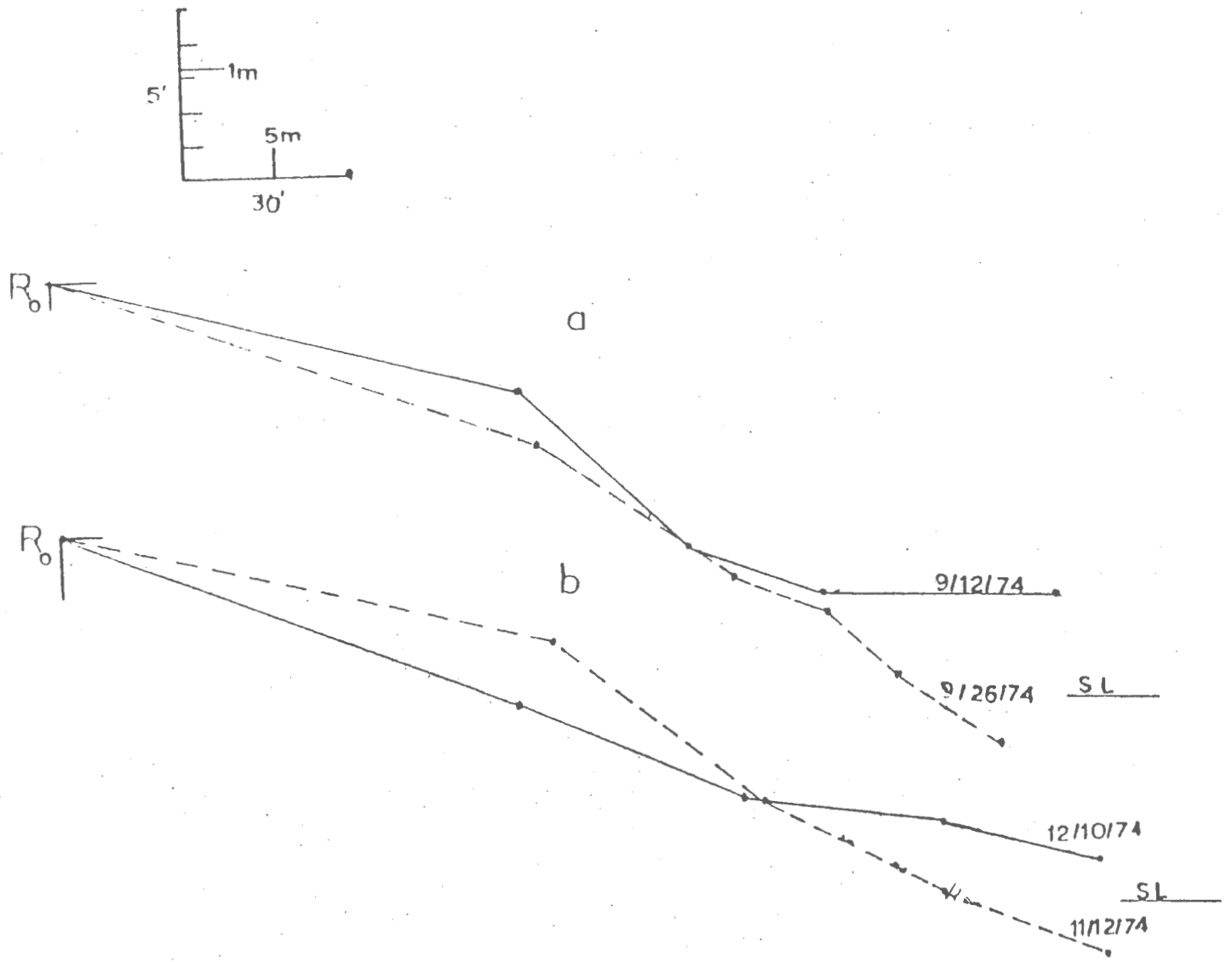
1m
5'
5m
30'
R_o
a
R_o
b
9/12/74
9/26/74
SL
12/10/74
SL
11/12/74

Figure 6. The non-uniform behavior of the observational beaches under the same wave conditions. The profiles indicate Green Hill is accreting while East and Weekapaug are eroding in this time span.

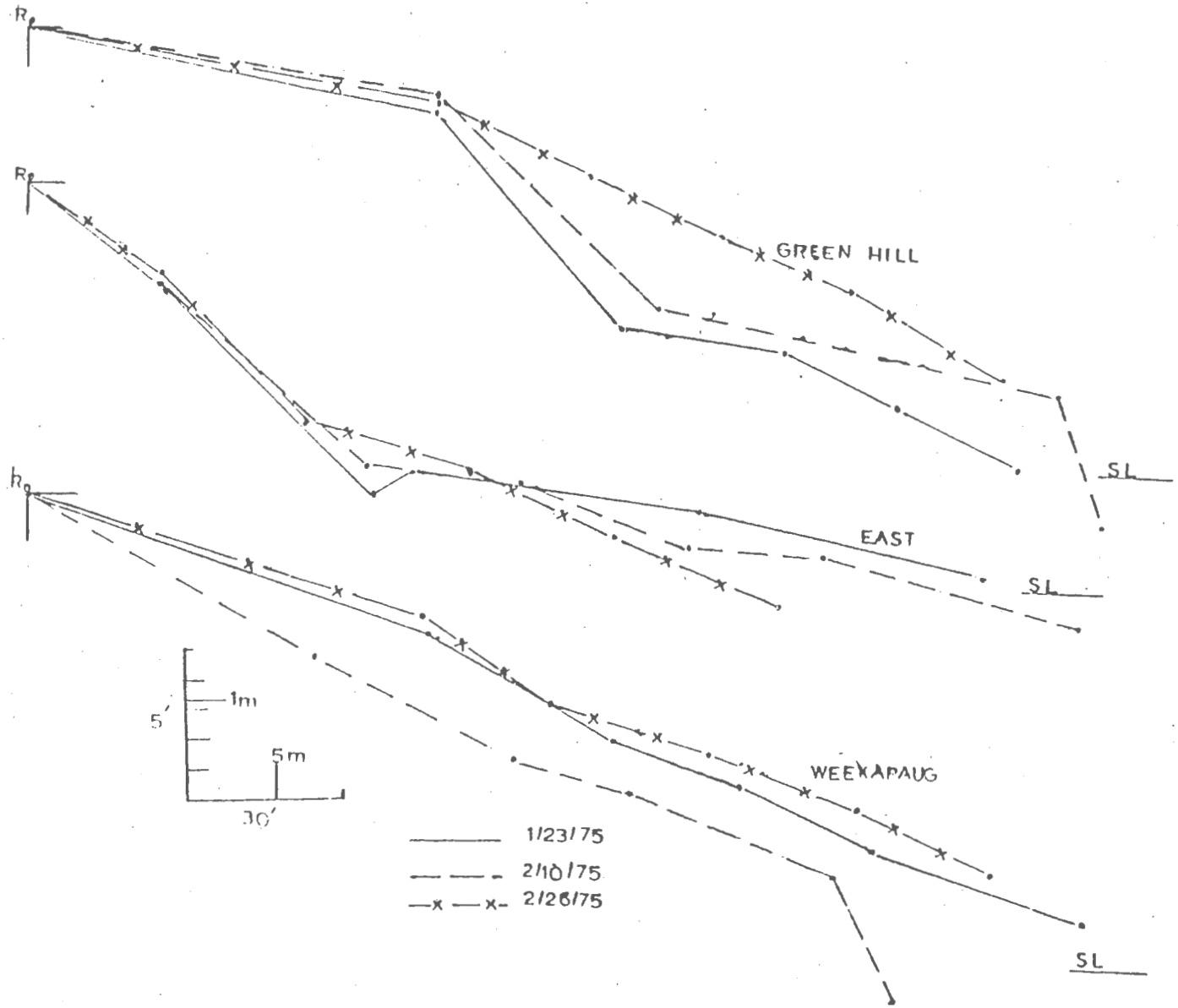
R
R
h
GREEN HILL
SL
EAST
SL
WEEKAPAUG
SL
5'
1m
5m
30'
1/23/75
2/10/75
2/26/75

Offshore Profiles

In early September 1975 offshore profile pairs were made off Weekapaug and East Beaches. No offshore bars were observed on either of these profiles. Furthermore, contouring failed to indicate the occurrence of any significant bottom forms within the 0.3 m resolution of the sounding technique (Fig. 7). However the profiles were done after a building period so the sand may have been stored on the beaches.

Longshore Drift

The longshore drift was measured at about the same time in the tidal cycle for all beaches and correlated with wave characteristics (Table 3). Generally, speeds were fastest at Green Hill and slowest at East Beach. The computed speeds, however, did not indicate the variation between Green Hill and East Beach (Table 4 and Fig. 8). Also they tended to be somewhat higher than those observed and were equally as variable from beach to beach.

Longshore drift direction on any given day was compatible with wave direction and was the same at all three beaches. In one instance, though, the drift was counter to the wave approach and wind direction. Also, on two occasions, when the waves were propagating parallel to the beach, the drifter slowed and moved on a course perpendicular to the shore with no aid from the wind. This pathway was probably caused by a rip current.

May and Tanner Computer Output

Longshore Drift

The May and Tanner model (1973) predicts different drift directions for the beaches in 17% of the paired data from Tables 3 and 4.

Figure 7. Nearshore topography off Weekapaug and East beaches based upon sounding profile pairs. Contours in feet.

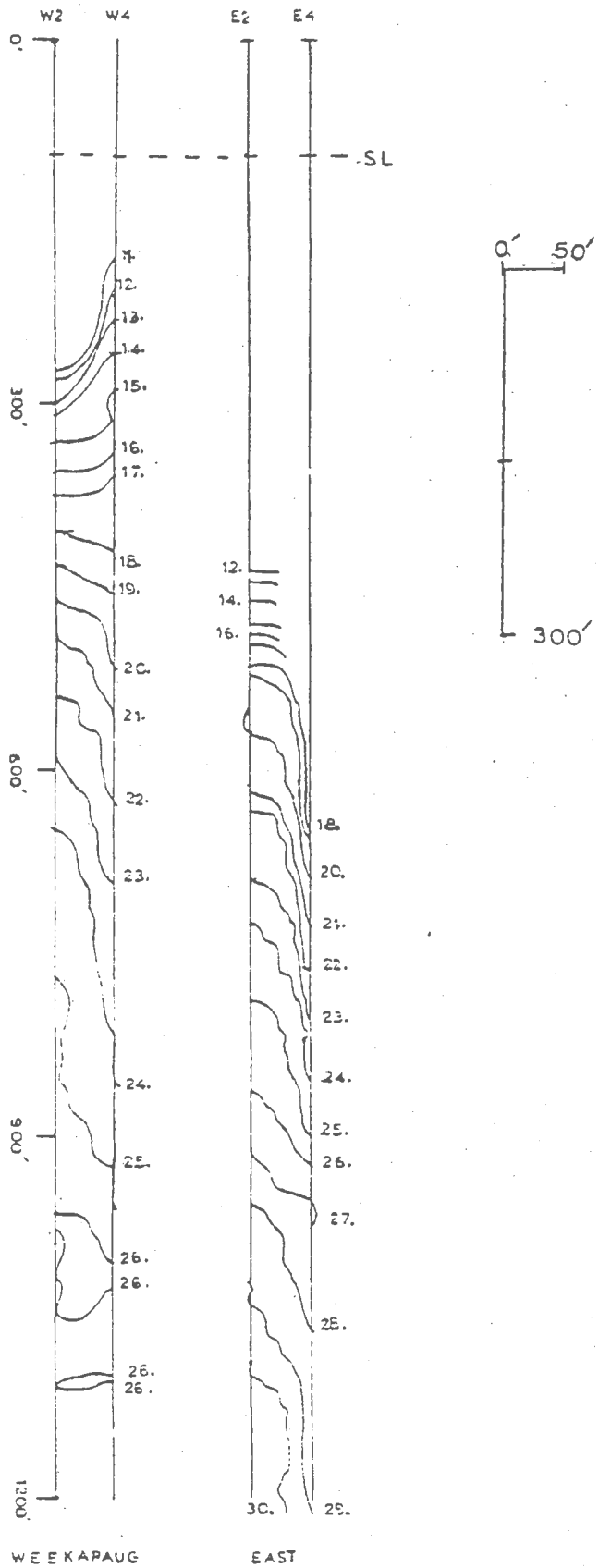
W2
W4
E2
E4
0'
SL
300'
600'
900'
1200'
11.
12.
13.
14.
15.
16.
17.
18.
19.
20.
21.
22.
23.
24.
25.
26.
26.
26.
26.
12.
14.
16.
18.
20.
21.
22.
23.
24.
25.
26.
27.
28.
30.
29.
0'
50'
300'
WEEKAPAUG
EAST

Table 3. Longshore Current Measurements

Date	Beach		
	Weekapaug (cm/s)	East (cm/s)	Green Hill (cm/s)
9/ 5/74	———	17.0 (W)	8.6 (W)
11/ 4/74	23.0 (W)	~23.0 (W)	~23.0 (W)
1/10/75	———	91.0 (W)	———
2/10/75	91.0 (E)	91.0 (E)	91.0 (E)
2/21/75	46.8 (E)	43.9 (E)	———
3/18/75	18.9 (W)	11.8 (W)	21.7 (W)
4/ 8/75	13.0 (E)	14.7 (E)	20.2 (E)
4/18/75	25.4 (W)	20.2 (W)	25.8 (W)
5/ 6/75	7.1 (W)	6.5 (W)	12.4 (W)
7/29/75	7.6 (E)	22.0 (E)	———
9/27/75	———	15.3 (W)	13.6 (W)

Table 4. Predicted Longshore Velocities

Date	Beach		
	Weekapaug (cm/s)	East (cm/s)	Green Hill (cm/s)
9/ 5/74	———	16.0 (W)	24.0 (W)
11/ 4/74	———	~55.0 (W)	55.0 (W)
1/10/75	29.0 (W)	~55.0 (W)	13.0 (E)
2/10/75	~10.0 (E)	33.0 (E)	24.0 (W)
2/21/75	~70.0 (E)	~17.0 (E)	4.0 (W)
3/18/75	33.0 (W)	~55.0 (W)	200.0 (W)
4/ 8/75	~10.0 (E)	33.0 (E)	24.0 (W)
4/18/75	12.0 (W)	38.0 (W)	10.0 (W)
5/ 6/75	———	48.0 (E)	24.0 (W)
7/29/75	4.0 (W)	17.0 (W)	~15.0 (W)
9/27/75	41.0 (E)	33.0 (W)	———

Figure 8. Observed and predicted longshore current velocities (cm/s).

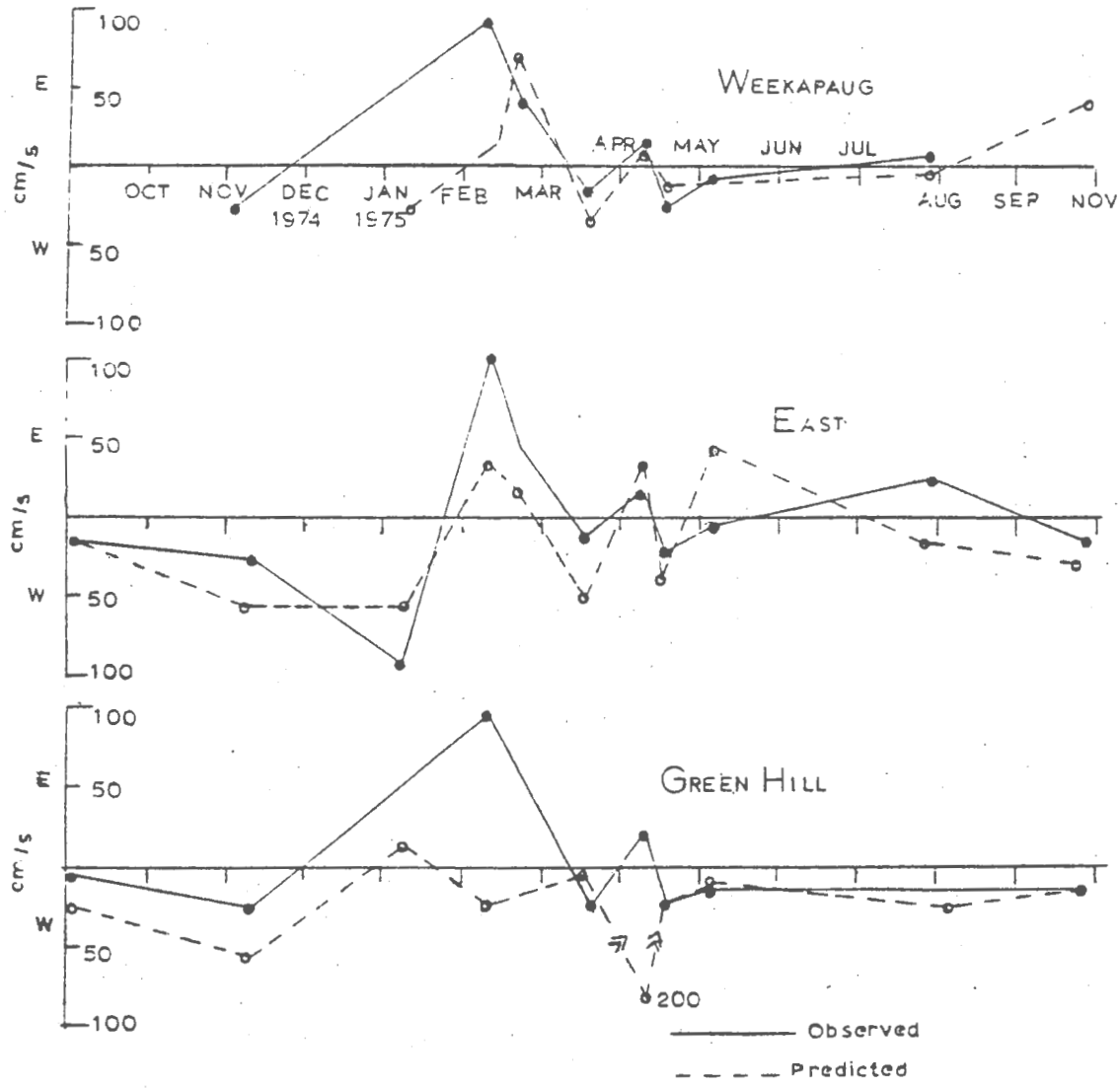
WEEKAPAUG
EAST
GREEN HILL
E
W
cm/s
100
50
OCT
NOV
DEC
1974
JAN
1975
FEB
MAR
APR
MAY
JUN
JUL
AUG
SEP
NOV
200
Observed
Predicted

More importantly however these data suggest an extensive pattern of converging and diverging directions along the coast.

Since the littoral component of wave power (P_L) is directly proportional to the incident angle β, the resulting P_L values can either be positive or negative, depending upon whether β is greater or less than 180°. Therefore when a P_L curve is drawn on an x-y coordinate system, it may cross and recross the zero line several times over the distance of the shoreline. When the curve lies on the positive side of the zero line, longshore drift is arbitrarily designated as eastward and westward if it is below the line. As a result of subjective decisions, more cells were indicated when the P_L curves followed the zero line closely.

Drift directions and lengths along the shore are illustrated by using southwest (200°T), normal (160°T) and southeast (120°T) approach angles at H = 0.1 m, T = 6 s (Pl. 1). For southwest waves (200°T) several eastward and westward movements (∿0.5 km) occur on the windward sides of headlands, while to leeward 2 to 6 km long eastward drifts are generated (Pl. 1). Waves approaching normal to the shore (160°T) produce two larger cells (1 to 3 km) on both sides of the headlands with smaller cells (∿0.2 km) in the bays. Waves having a southeast approach (120°T) show short (∿0.5 to 1.0 km) east-west drifts on the windward side of Quonochontaug. Immediately west of Quonochontaug Point and Charlestown Breachway, westward drifts of 5 km and 2 km, respectively occur with a 1 km eastward drift in the bay between Charlestown and Green Hill.

Comparison

Beach Profile and May and Tanner Erosion-Accretion Potential (ΔP_L)

At Weekapaug, East and Green Hill Beaches three selected sets of beach surveys and wave data were used to check the accuracy of the May and Tanner (1973) model predictions regarding deposition and erosion. The model output included the computed longshore wave power (P_L) and the corresponding longshore gradient (ΔP_L) for the Weekapaug Point to Green Hill Point coastline for selected ranges of wave angles, periods, and heights in all possible combinations (Table 5) (Pl. 2-6). This method was used because the breaker position versus breaker power did not provide the necessary insights into the causes of the different response styles (Appendix B) and the attempt to predict seasonal beach accretional-erosional cycles were unsuccessful (Appendix C). The first set of observations and measurements considered for the beaches was on January 10, 17, 19, and 23, 1975. For the wave conditions and associated ΔP_L curves (Pl. 2-6) refer to Table 6. On January 10 the waves were southeasterly, and a week later on January 17 southwesterly waves were observed.

The Weekapaug Beach surveys of January 10 and 17 indicated accretion (Fig. 9) had occurred while the appropriate ΔP_L curves suggested erosional condition. On January 19 south-southwest waves were observed and the appropriate ΔP_L curve for the January 19 conditions suggested a cutting back of the beach just as the profiles indicated. For January 23 waves were approaching from the southeast and the ΔP_L curve appeared to indicate erosion which the survey showed took place on the foreshore (Fig. 9). However, the deposition on the backshore was not predicted by

Table 5. Wave Parameters for P_L Plots

Period (s)	4		6		9	
Height (m)	0.1	1.5	0.1	1.5	0.1	1.5
Angles (^{o} T)	200	200	200	200	200	200
	180	180	180	180	180	180
	160	160	160	160	160	160
	140	140	140	140	140	140
	120	120	120	120	120	120

Combinations of height, period, and approach angle for the longshore power curves.

Table 6. Wave Conditions and Corresponding ΔP_L

Date (1975)	Wave Conditions	Corresponding ΔP_L
January 10	134°T, H=0.1-0.3m, T=6s	140°T, H=0.1m, T=6s
January 17	200°T, H=0.3-0.6m, T=4s	200°T, H=0.1m, T=4s
January 19	190°T, H=0.6-0.9m, T=6s	200°T, H=1.5m, T=6s
January 23	160°T, H=0.1-0.3m, T=6s	160°T, H=0.1m, T=6s
Weekapaug		
July 29	160°T, H=0.3-0.6m, T=7s	160°T, H=0.1m, T=6s
August 22	214°T, H=0.6-1.2m, T=6s	200°T, H=1.5m, T=6s
East		
July 29	166°T, H=0.6-1.2m, T=7s	160°T, H=1.5m, T=6s
August 22	210°T, H=0.9-1.5m, T=5.5s	200°T, H=1.5m, T=6s
Green Hill		
July 29	200°T, H=0.6-0.9m, T=6.5s	200°T, H=1.5m, T=6s
August 22	210°T, H=0.6-1.2m, T=4.5s	200°T, H=1.5m, T=4s
January 23	160°T, H=0.1m, T=6s	160°T, H=0.1m, T=6s
February 10	200°T, H=0.1m, T=5s	200°T, H=0.1m, T=4s

Figure 9. Profiles of Weekapaug, East, and Green Hill beaches for January 10 to January 23, 1975. These show the elevation changes that occurred and are used in the comparison with the appropriate ΔP_L curves in Table 6.

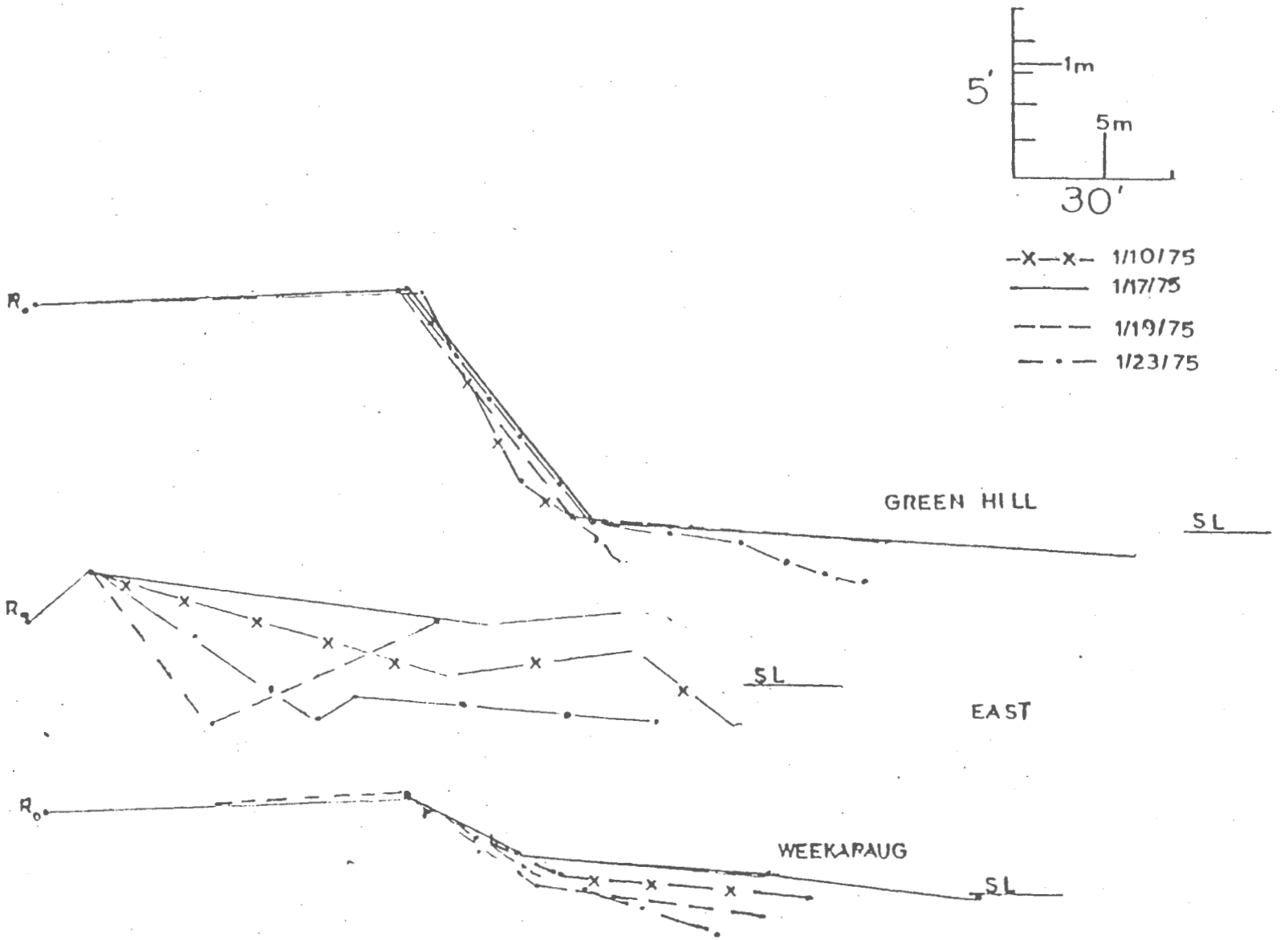
5'
1m
5m
30'
-x-x- 1/10/75
1/17/75
1/19/75
1/23/75
R
GREEN HILL
SL
R
SL
EAST
R
WEEKAPAUG
SL

the ΔP_L curve. It should be noted that for all three chronological responses the only data used to choose the appropriate ΔP_L curves were based upon observations taken when the beach surveys were conducted and the selected ΔP_L curves were not weighted because the duration of specific wave conditions was not known. Therefore any shifts in the wave regimes between the survey dates were not measured and hence not incorporated into the selection process.

Similar analyses employing the same wave information base were undertaken for East and Green Hill Beaches. The sequence of beach responses for each of these beaches was the same as that recorded at Weekapaug for the specified dates. Furthermore, at these beaches the predicted responses from the appropriate ΔP_L curves and observational responses were inclined to agree for each date with the exception of the depositional events on the backshores.

Summarizing this first set of examples, all three beaches responded in the same manner under the stated wave regimes. Moreover in most cases the associated ΔP_L curves tended to successfully predict the simple deposition or erosion response but was unable to indicate the compound response of erosion on the foreshore and deposition on the backshore.

The second set of examples was composed of wave conditions and beach surveys of July 29 and August 22, 1975. On July 29 the waves were approaching from the southeast (Table 6). For three weeks of the study period no wave conditions were observed, so hindcasting was employed and generated southwest waves with a 6 s period and 0.6 m height. This was done to get a feeling for the general direction of wave approach and significant height and period for the wind conditions.

However, for consistency hindcasting was not used in choosing a ΔP_L curve for response comparisons. By August 22 the waves were observed to be approaching from the southwest.

For all three beaches the ΔP_L curves indicated an erosional response. This prediction adequately modeled the response of Weekapaug and East Beaches but not that of Green Hill. The surveys of July 29 and August 22 showed erosion on the foreshore and building on the backshore (Fig. 10). In summary, the model successfully predicted the sole erosional response of Weekapaug and East Beaches but was unable to designate the combined reaction measured at Green Hill.

A final set of examples was chosen specifically to examine the model's capability for predicting opposing beach changes under a given set of wave conditions. For this purpose the January 23 and February 10, 1975 surveys were selected when the wave conditions were southeasterly and southwesterly, respectively (Table 6). The surveys for Weekapaug and Green Hill showed erosion and building responses respectively (Fig. 11) but the model indicated both simple responses to be erosional. Furthermore at East Beach the model predicted the same erosional response but the surveys indicated deposition on the backshore and erosion on the foreshore. Thus, these examples demonstrated that under the same wave conditions, the model was not able to predict correctly this a non-uniform response. For this set of examples Weekapaug was cut-back, East Beach both eroded and accreted, and Green Hill built-up.

Figure 10. Profiles of Weekapaug, East, and Green Hill beaches for July 29 to August 22, 1975. These show the elevation changes that occurred and are used in the comparison with the appropriate ΔP_L curves in Table 6.

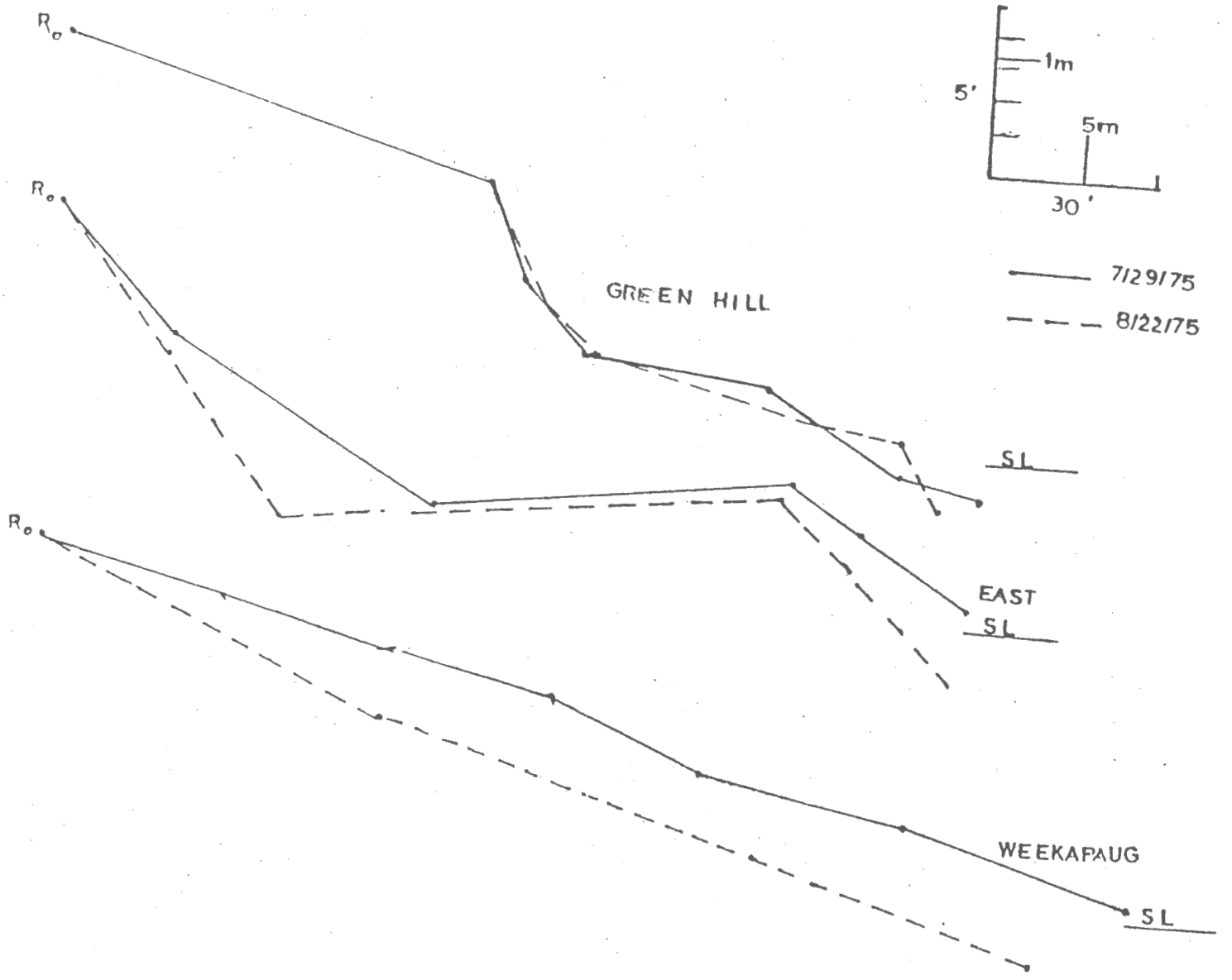
R_o
R_o
R_o
GREEN HILL
EAST
WEEKAPAUG
SL
SL
SL
1m
5m
5'
30'
7/29/75
8/22/75

Figure 11. Profiles of Weekapaug, East, and Green Hill beaches for January 23 to February 10, 1975. These show the elevation changes that occurred and are used in the comparison with the appropriate ΔP_L curves in Table 6.

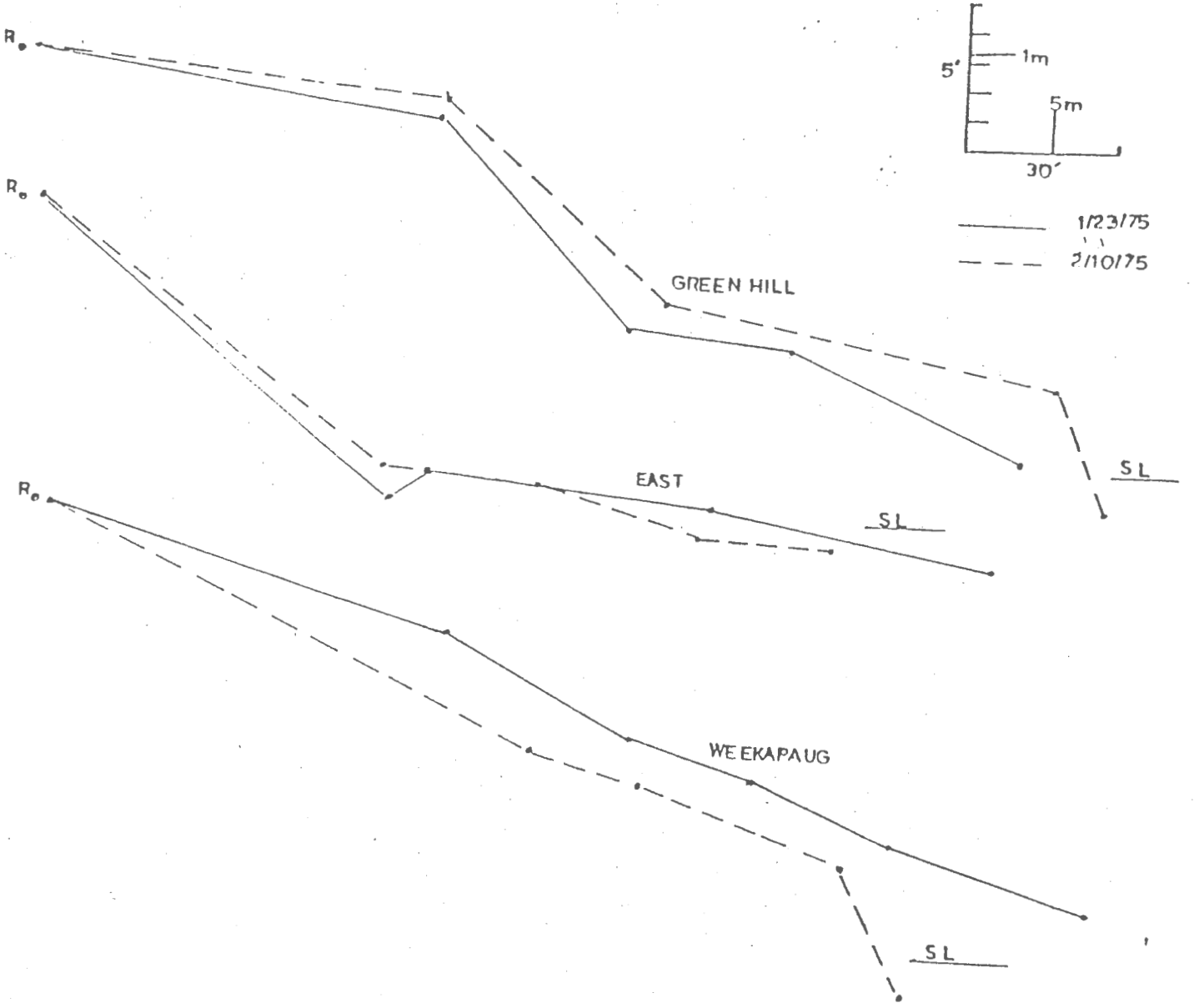
5'
1m
5m
30'
1/23/75
2/10/75
GREEN HILL
EAST
WEEKAPAUG
SL
SL
SL

VI. DISCUSSION

Waves and Beach Response

For the southwestern Rhode Island shoreline the wave direction was found to have a general relationship with beach erosional and depositional response. Waves from the southwest usually caused the beaches to build out, whereas southeasterly waves were ordinarily responsible for the loss of beach sand. However, field data indicated there were times when southwest waves caused erosion, and southeast waves, deposition. For example, southwest waves with $H \geq 1$ m and $T \leq 6$ s created an eroding environment in January for all three beaches, and southeast waves of $H \leq 0.6$ m and $T \geq 8$ s promoted building at Green Hill in October.

Assuming a smoothed and simplified bottom topography, refraction sketches (Figs. 12-14) are drawn for wave approach angles from the southwest (225°T) and southeast (135°T) at the three beach half re-entrants. In these half re-entrants the inflection points (a, b, c, d, and e) are located. Under a southwest wave attack Weekapaug is eroding (Fig. 12a). The erosion, however, is of small magnitude as the beach is in close proximity to point c. East Beach (Fig. 13a) is undergoing deposition of large volumes of sand. This is occurring because the beach lies near point d, the maximum deposition point. Green Hill Beach (Fig. 14a) is being eroded because it is close to point c. For the southeasterly attack Weekapaug and Green Hill are not found on the depositional side of point c, while East Beach is in the area of maximum erosion. Significantly, East Beach has a large response, while Weekapaug's is small and Green Hill's is intermediate. Both the response and the gross magnitude of the response are confirmed by the beach surveys.

Figure 12. (a) Refraction sketch of southwest and southeast wave rays at Weekapaug. Included in the diagram is the placement of inflection points (a-e) used in the May and Tanner (1973) model.

(b) Refraction sketch of southwest wave rays shifted $\pm 5^{o}$ at Weekapaug.

(c) Refraction sketch of southwest wave rays shifted $\pm 5^{o}$ at Weekapaug.

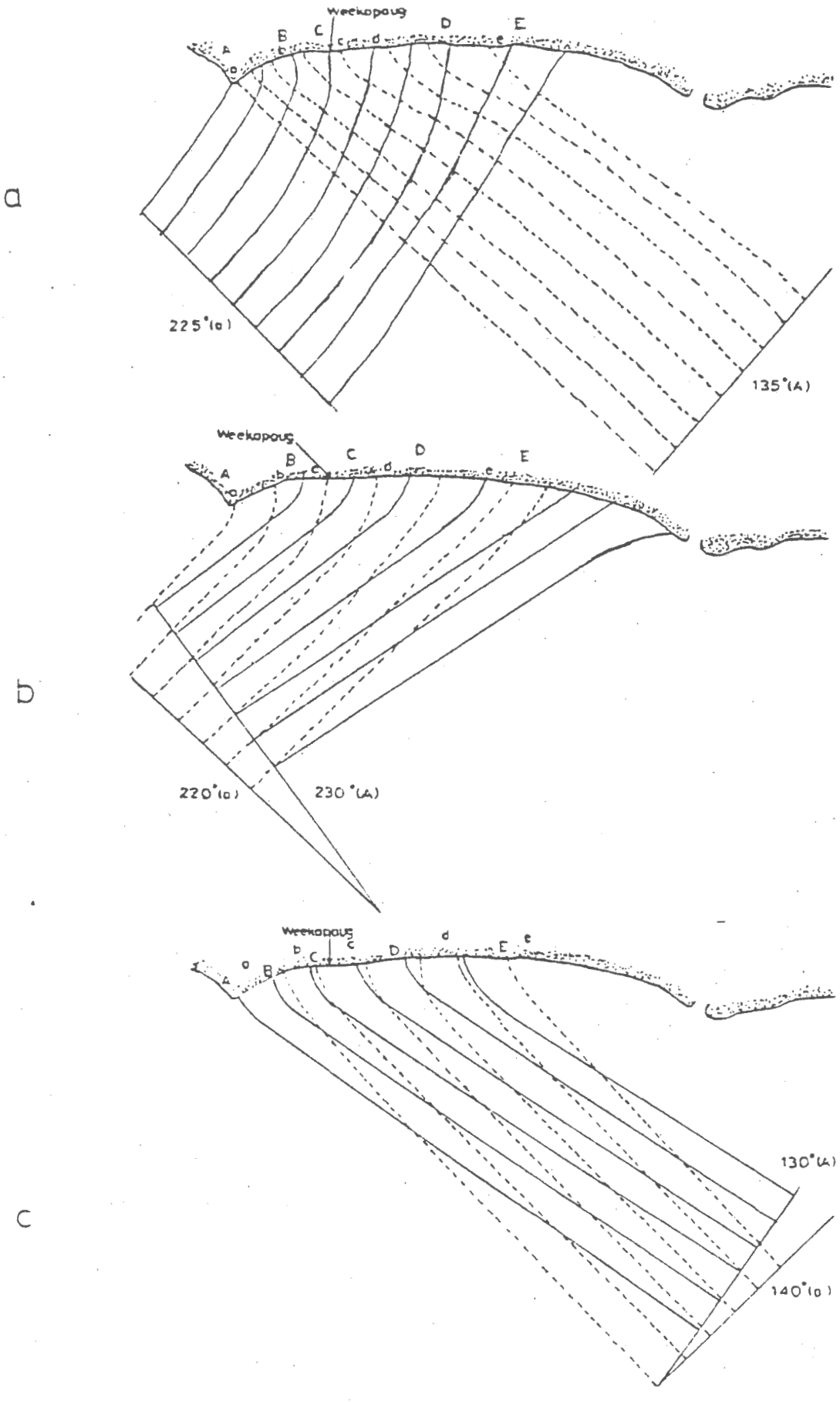
a
Weekapaug
A
B
C
D
E
225°(a)
135°(A)
b
Weekapaug
A
B
C
D
E
220°(a)
230°(A)
c
Weekapaug
A
B
C
D
E
130°(A)
140°(a)

Figure 13. (a) Refraction sketch of southwest and southeast wave rays at East Beach. Included in the diagram is the placement of inflection points (a-e) used in the May and Tanner (1973) model.

(b) Refraction sketch of southwest wave rays shifted $\pm 5^{o}$ at East Beach.

(c) Refraction sketch of southeast wave rays shifted $\pm 5^{o}$ at East Beach.

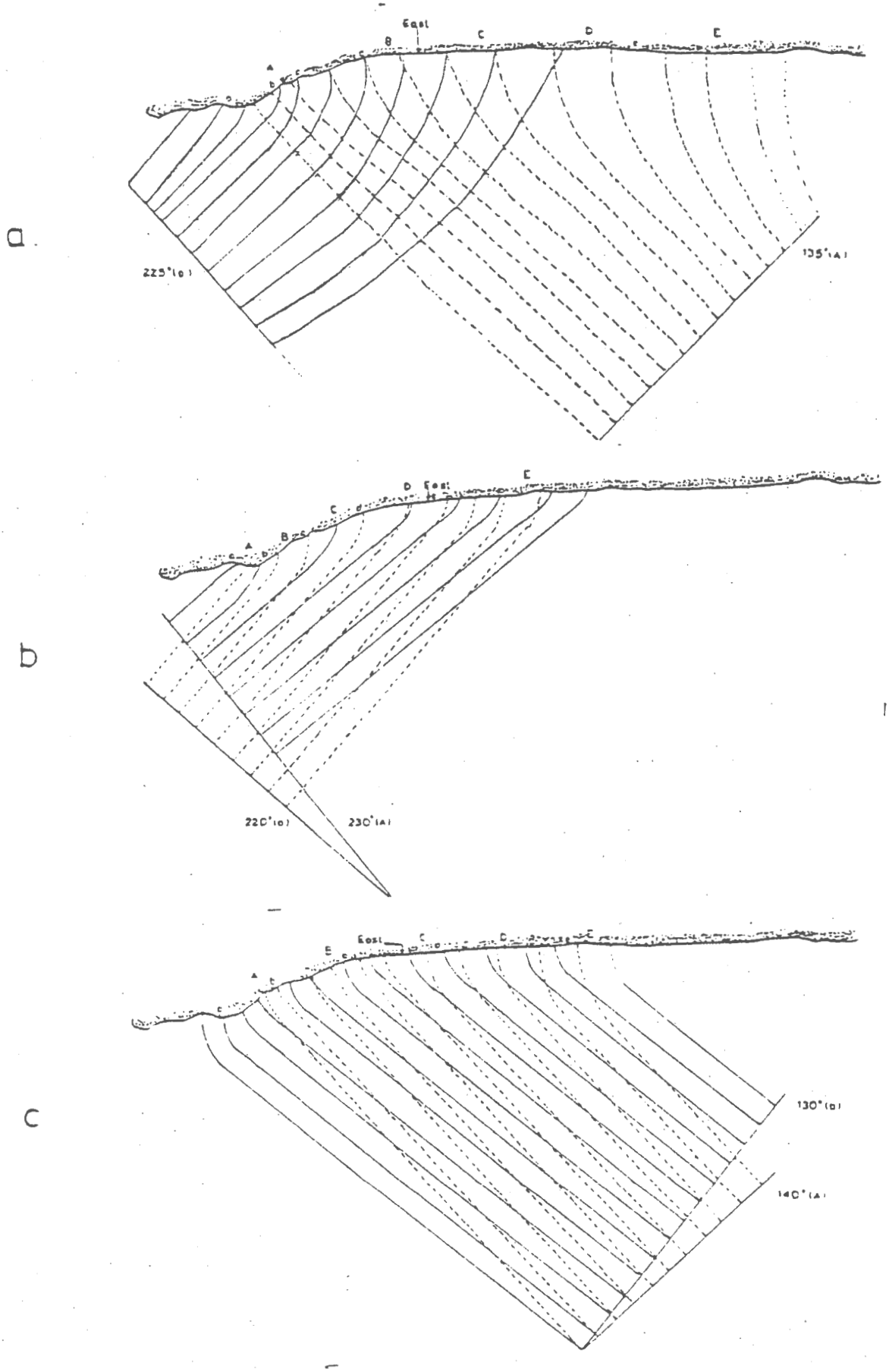
a
East
A
B
C
D
E
225°(a)
135°(A)
b
East
A
B
C
D
E
220°(a)
230°(A)
c
East
A
B
C
D
E
130°(a)
140°(A)

Figure 14. (a) Refraction sketch of southwest and southeast wave rays at Green Hill. Included in the diagram is the placement of inflection points (a-e) used in the May and Tanner (1973) model.

(b) Refraction sketch of southwest wave rays shifted $\pm 5^{\circ}$ at Green Hill.

(c) Refraction sketch of southeast wave rays shifted $\pm 5^{\circ}$ at Green Hill.

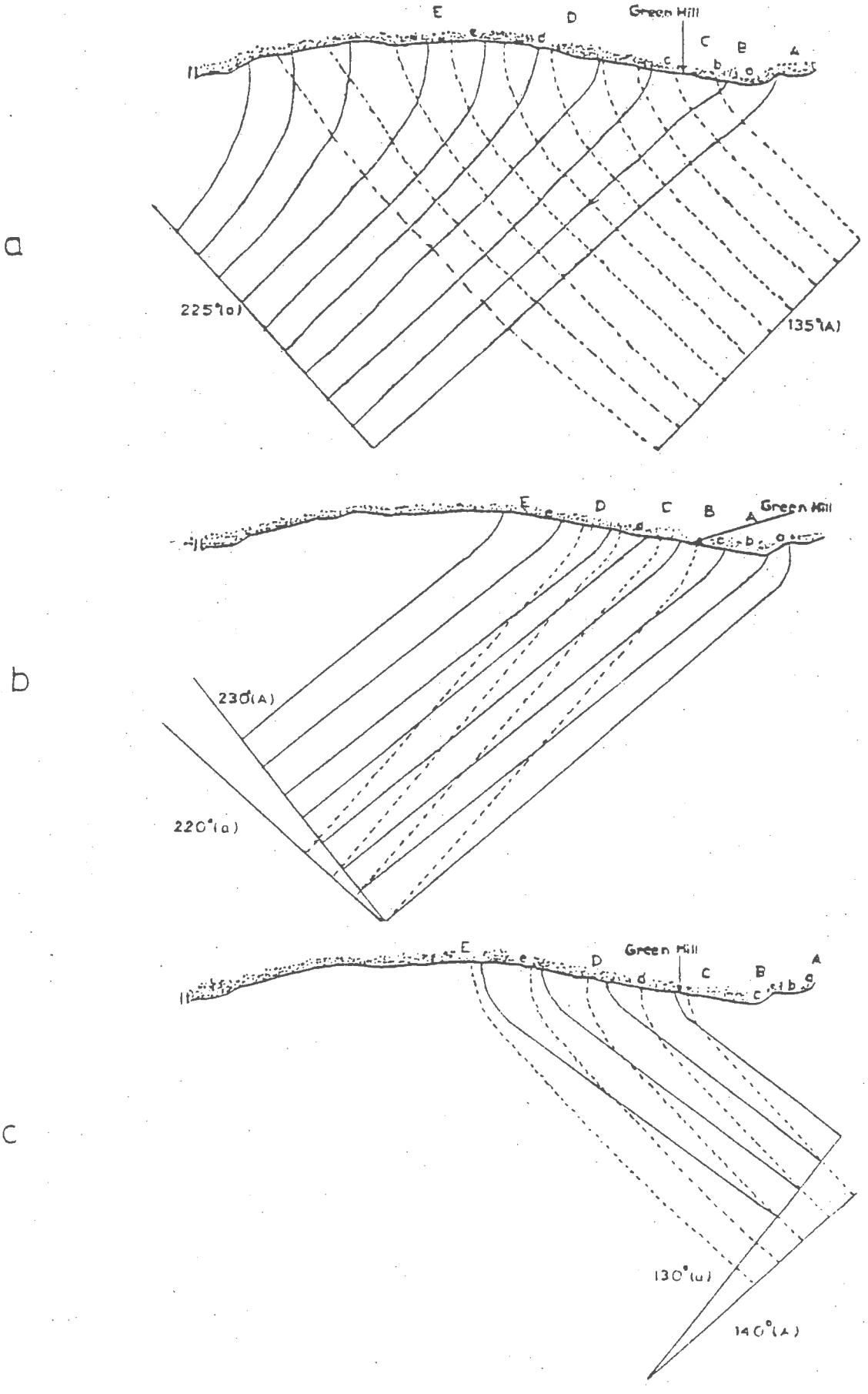
a
E
D
Green Hill
C
B
A
225°(a)
135°(A)
b
E
D
C
B
A
Green Hill
230°(A)
220°(a)
c
E
D
Green Hill
C
B
A
130°(a)
140°(A)

The importance of slight variations in wave approach and the corresponding changes in refraction patterns are explored by altering the basic wave direction by $\pm$ 5° (Figs. 12b,c-14b,c). For Weekapaug the sketches reveal eroding events for the 140°T and 230°T directions while the 130°T and 220°T directions are associated with building. Point c is always very close to Weekapaug. For East Beach (Fig. 13b,c) all southwest directions and 140°T indicate deposition in varying magnitudes with erosion occurring for 130°T. The variations may explain why the berm at East Beach did not recover as quickly as expected from the December 1, 1974 storm since the wave regimes may have shifted enough so net deposition was small. For Green Hill (Fig. 14b,c) and 230°T shows maximum erosion while 130°T, 140°T, and 220°T directions indicate deposition of varying magnitudes.

A summarization of the results of the refraction sketches is presented in Table 7. Of the six angles selected, only one (220°T) resulted in a uniform response.

Clearly, small variations in approach direction can cause significant differences in the behavior of beaches. In order to get a uniform depositional response, it appears that the refraction along the coastline must be centered on the headlands so that most of the energy approaching the re-entrant is expended on these headlands leaving only the energy required for deposition. Thus the longshore current loses its ability to entrain and transport sediment and the sand is deposited on the beaches. In order for this to occur the refraction around the headlands of Weekapaug and East must concentrate the highest energy to the east of the point so the wave rays quickly spread to favor deposition.

Table 7. Beach Response as a Function of Wave Direction

Wave Direction	Beaches		
	Weekapaug	East	Green Hill
130°T	d*	e*	d
135°T	d	e	d
140°T	e	d	d
220°T	d	d	d
225°T	e	d	e
230°T	e	d	e

* d is deposition and e is erosion.

At Green Hill the highest energy concentrates to the east of the Point so as to create a depositional regime toward the west.

Conversely, within the re-entrants, the uniform erosional response is a result of the refracted wave rays converging so each beach is in the high energy area. However, it must be noted that the uniform response case is probably not unique since only a few approach angles are sketched. Furthermore other wave parameters, and the complex nearshore topography are also not considered.

The non-uniform behavior results when the refraction, as a result of the original angle, creates a zone of concentrated energy at each headland. Thus the re-entrant configuration will refract the wave rays and spread the energy so the erosional and depositional areas are in unique places within the respective re-entrants. For example 130°T shows East Beach undergoing erosion and Weekapaug and Green Hill deposition.

Circulation Cells

For sometime it has been recognized that nearshore circulation cells are driven by difference in mean water level along the shoreline (Inman, 1960). Waves travelling toward the shore induce a second-order pressure field causing the mean water level to set-down outside the breaker zone and set-up inside the zone. This condition produces a ridge and valley-like envelope parallel to the shore. Furthermore, wave refraction over irregular offshore topography promotes wave height changes along the beach that cause the mean water level to vary resulting in a longshore gradient within the surf zone. Thus, flow in the form of littoral currents moves laterally from areas of high waves

(higher set-ups) to low waves (lower set-ups) and turns seaward as rip currents where breakers are lower.

Breaker heights were calculated data provided by the May and Tanner (1973) program and as such were dependent upon the refraction, shoaling, and refraction coefficients. A plot of the breaker heights along the coastline were used to sketch apparent circulation cells for three different angles of wave approach (Pl. 7). These cells were the result of subjective decisions made regarding significant height differentials. At Charlestown Breachway the projective jetties were included as part of the shoreline configuration, but these structures could not be handled by the program and therefore the model was unable to calculate reasonable breaker heights at this location.

Waves advancing from the southwest direction (200°T) generate cells ranging from 0.2 km to 3.0 km long. Smaller cells are stacked-up on the western side of the headlands, where the wave orthogonals are most nearly normal to the shoreline. The larger cells occur to the east of these headlands and in the bays (Pl. 7) where the orthogonals are nearly parallel to the coastline. For the approach normal (160°T) to the shore, cells between 0.2 km and 2.0 km are evenly distributed alone the coastline with no stacking at promontories. Two of the largest cells (2.0 km) are in the bay between Weekapaug and Quonochontaug Points while the other large cell (2.0 km) is between Charlestown and Green Hill. Waves from the southeast direction (120°T) produce cells ranging from 0.2 km to 4.0 km. The smaller cells tend to stack on the eastern side of Quonochontaug Point and appear to be grouping on eastern side of Green Hill, while the larger cells are to the west of the headlands. Thus small cells are clustered on the windward sides of shoreline

projections for waves from the southwest and southeast, but these cells do not occur when waves arrive perpendicular to the coastline.

Although May and Tanner (1973) did not choose to derive a nearshore circulation system from their model, the computed directions of longshore currents, that are dependent upon wave incident angle (β) but independent of breaker height, were applied to construct apparent nearshore circulation within the surf zone. These P_L curves are smooth, undulating curves. To construct the apparent cells, an arbitrary amplitude and minimum distance along the shore was used. For small amplitudes and/or short longshore distances an element of uncertainty existed as to how real were the reversals, so these were included in the larger 'cells'.

Waves from the southwest (200°T) produce small (0.5 km) cells that are grouped on the western sides of promontories (Pl. 1), while the larger cells (2 to 6 km) occur on the leeward side of the headlands. When waves are directed perpendicular (160°T) to the shore, small cells ($\sim$0.2 km), as well as large (1 to 3 km) ones, form in the bays. Cells (1 to 3 km) occur at Quonochontaug Point. Waves from the southeast (120°T) generate small cells ($\sim$1 km) that are on the eastern side of Quonochontaug headland with larger cells (2 to 5 km) developing in the bays.

Thus nearshore circulation patterns produced by longshore changes in wave breaker heights and longshore current directional variations, are similar relative to cell types and occurrences, but differ in terms of cell size and specific location. However, the reality of the cells and the criteria used to generate them need substantiation from field observation.

Longshore Currents

The field data indicated the longshore currents to be fastest at Green Hill, slower at Weekapaug, and slowest at East Beach. In seeking an explanation for the differing current speeds, nearshore bathymetry is considered to be a prime factor (Fig. 1). Of the three modes by which longshore currents are generated; an oblique wave approach, wave set-up and set-down, and differential breaker height (Komar, 1974), differential breaker height and wave set-up and set-down best reflect the importance of bathymetry. Also westward flowing tidal currents, 25 to 55 cm/s and eastward moving ebbing flow may have some effect on the resulting longshore currents.

To explain the longshore velocities at Green Hill, East Beach, and Weekapaug the cumulative effect of the waves and their interaction with offshore relief and shoreline configuration are considered specifically. Green Hill is less than 1 km from its headland which focuses the wave orthogonals in accordance with refraction. As a result, the high waves cluster creating a wave set-up and a high potential longshore hydraulic gradient. Thus water in the form of longshore currents flows away from the headland toward sites of lower wave set-up. The relative positions of the beach on the gradient will cause the development of a swift longshore current.

Although similar waves occur at East Beach the local hydraulic gradient produces a slower longshore drift. East Beach is some 3 km from Quonochontaug Point and in that distance the flow gradient probably dissipated resulting in a slower current.

At Weekapaug the longshore drift is slightly faster than that at

East Beach. The flow rate is faster than expected because the beach is only 1.0 km from the headland and therefore occupies a higher position on the longshore flow gradient.

Evaluation of the May and Tanner Program

The May and Tanner (1973) model is based upon the Wilson (1966) refraction program and therefore certain innate constraints are imposed. The Wilson (1966) program, as that of Dobson (1967) is derived from the theory of linear progressive waves, which implies small wave steepness, constant depth and period, obedience to Snell's laws, minimal diffraction and reflection, and straight and parallel contours (Bryant, 1974). Such assumptions cause these genera of refraction programs to fail when complex shoals, rapid bathymetric changes, and breaking waves are involved (Fig. 1). However, even at this level of primitiveness Bryant (1974) was able to demonstrate that the Wilson (1966) refraction program approximates the conditions at the shoreline. Therefore a reasonable representation of actual refraction patterns can be described.

Affecting the refraction pattern is the grid depth representation or the number of grid units in both the x and y directions used to define the underwater topography. Hence, a small number of grid units will generalize the bathymetric character but very often significant features such as shoals will be lost. For the present study the grid size (0.1 km by 0.1 km) is found to be adequate for the description of the bottom topography.

Assuming a large unit grid size (1 km by 1 km) lateral coastal energy patterns become generalized as do the inferred circulation cell patterns. Moreover, breaker energy peaks (Appendix D) may also appear

anomalous. Part of these problems may be alleviated by spacing the wave rays at partial grid units. Thus circulation patterns became less general and smaller cells emergy. Moreover the breaker energy peaks will appear less erratic due to the increased number of wave rays. Therefore any interpretation of P_L, ΔP_L, and circulation curves must include consideration of the grid size and wave ray saturation.

A somewhat subtle implication of the grid size or bottom surface description is the ability of the model to predict wave heights. The model employs equation 18 (p. 52, May and Tanner, 1973) to recalculate the wave height at any point along the wave ray by considering the original height, refraction coefficient, wavelength, and depth in a hyperbolic geometric function, as well as the past history of the wave. This history is comprised of an integral which in itself is a complicated function of the period, bottom friction coefficient, wavelengths, depths, and calculated heights. It is the latter part of the equation, utilized in its discrete form; i.e., $-0.67 \sum_{i=1}^{i} (x_j - x_{j-1})(Tc_f\sigma^3 H_j^2/(L_j \pi \gamma \sinh^3(k_j h_j)))$ which allows the model to better approximate natural conditions by considering the bathymetry. This study finds that wave heights calculated by the model are in acceptable agreement with those measured at the beaches. Recently Tanner (1976) has indicated that waves generated by the program are about 35% higher than field observations. The reason for this difference is that the program allows for only one breaking episode and no provisions exist for waves to reform.

A result of one breaker zone is that the longshore current velocities predicted by the model are too high when compared to the observed current (Appendix E). The discrepancy between the predicted and observed velocities results from the dissipation of the hydraulic head

in the natural system (Shepard and Inman, 1950). Both alternating sets of high and low waves, and rip currents have been demonstrated to be the causal mechanisms of this dissipation.

In the natural system the alternations of wave height sets produce a variation in the amount of energy delivered to the longshore current over time. The model ignores this complexity because the output is based upon a single set of wave conditions at a given instant in time and generates its longshore current by angle β only. Rip currents lessen the hydraulic head by transporting water offshore thus reducing the longshore velocities almost to zero. Although rip currents are predicted indirectly by the model, they are not actively considered by the model.

The model uses the variation in longshore velocities to delineate potential depositional and/or erosional sites along a coastline. These currents are driven by breakers which are dependent on wave energy density and breaker angle (Komar, 1974). Bagnold (1963, 1966), relates this energy to I_L, a sand transport rate. I_L, in turn, can be used to determine the volume transported, S_L (Inman and Bagnold, 1963). In Appendix F I_L and S_L have been calculated and indicate the model adequately approximates the volume of sand transported.

The model is developed for coasts with beach re-entrants. If the coast is regular the response potential (dq/dx) would be transportation rather than deposition or erosion. This is because P_L = constant and hence dq/dx = 0 for a straight beach. When dq/dx = 0 transportation is indicated.

Hindcasting was significant for the program in that is provided additional useful wave data. The hindcasted waves indicated a somewhat

wider range of wave characteristics than were observed, and therefore a better selection of wave parameters was made for P_L and ΔP_L. However, weighting of hindcasted waves was as difficult as with observed waves. Consequently in selecting ΔP_L curves for predicting beach responses the same problem arises as to which wave regime was more important during a specific time interval.

Other limitations are those related to the interpretation of the ΔP_L curves. While indicating where potential erosion and/or deposition may occur, the curves represent only a plan view and not a three-dimensional one. As the vertical dimension is not considered, on- and offshore sand migration appears to be ignored as a distinct process. Such sand movement seems to be largely responsible for observed beach foreshore configurations. Nevertheless, because the processes of on- and offshore sand movement and littoral sand transport cooperate in either storing or removing beach sand (Swift, 1976), the model by coincidence turns out to be successful in the two dimensional plan view.

Although the model correctly predicts uniform, simple erosional or accretional responses for a moderate energy coastline, it does not forecast compound responses of fair-weather and storm seasonal changes. In order to predict a compound response continuous wave and sea level positions are needed between the surveys. However even if continuous wave and sea surface data had been taken the model can only use discrete events of the continuous data and is not sophisticated enough to give a compound prognostication.

The fair-weather wave season is expected to produce an accretional event on the beaches (Appendix C). Unfortunately the derived seasonal

wave regime does not generate the proper ΔP_L curve (i.e., potential deposition) which identifies with this specific elevation change. Evidently one storm causes enough sand movement so that the prediction is incorrect. Also a large number of wave conditions must be considered for a better prediction. Finally the breaker energies could not be positively correlated with the response style, because the angle β upon which ΔP_L is based is not considered. Therefore, the model should only be used in the manner suggested by May and Tanner (1973). However, given an appropriate wave input based upon a predicted weather pressure system, the model will probably forecast a correct response in a reasonable number of cases.

VII. SUMMARY

1. As Weekapaug, East and Green Hill Beaches lie in three shoreline re-entrants, the May and Tanner (1973) model is generally successful in predicating simple erosional and/or depositional effects at these beaches. Thus, the model's application can be extended from West Florida's low energy coastline to a moderate energy shoreline typified by the southern Rhode Island beaches.

2. Uniform and non-uniform responses as well as their approximate magnitudes can be illustrated by simplified wave refraction diagrams in the three distinct beach re-entrants. These diagrams show that the half re-entrant inflection points (a,b,c,d, and e) shift in a non-systematic manner in response to different wave approach angles thereby causing the positions of beach erosion and deposition to change within each re-entrant.

3. Although no field observations were attempted to record nearshore circulation cells, the May and Tanner (1973) model's P_L curves as well as the computed wave height differentials alongshore suggest littoral drift reversals. However the numbers of littoral drift directional changes occurring in the field are expected to be less than those indicated by either the model's P_L curves or wave height differentials because of the subjectivity in selecting significant inflection points on the P_L curves or meaningful numerical differences in wave height along the shore.

4. No positive correlation is found between storm and fair-weather seasonal ΔP_L curves and their corresponding net seasonal changes in beach

elevations. During the fair-weather season, storm waves cannot be properly modeled unless a large spectrum of wave conditions are considered. Similarly in the storm season, the building waves cannot be considered for this same reason.

5. The May and Tanner (1973) model reveals several weaknesses. Longshore energy and drift directions are resolved in a scale pre-determined by the grid size. In addition the model tends to fail whenever a wave breaks offshore at rapid bathymetric changes and shoals and in the surf zone as there are no provisions for post wave breaking activity. Also the model forecasts wave heights and longshore velocities greater than actually measured because once waves break offshore which frequently occur in the study area, the model is incapable of considering regenerated smaller waves. For a regular shoreline, potential erosion-deposition predictions cannot be provided because the model only forecasts transportation ($dq/dx = 0$) for such a coastline. Finally, the model predicts cutting and filling in plan view, but does not give any indication of sand movement in the third dimension.

6. Measured longshore currents are fastest at Green Hill, slower at Weekapaug, and slowest at East Beach. In the vicinity of each beach observational station, the interaction of shoaling waves with local offshore topography and shoreline configuration produces a specific longshore hydraulic gradient. As these hydraulic gradients are expected to differ from beach to beach, the longshore current speeds should vary accordingly.

7. Intense southeast storm waves cause erosion at all beaches whereas moderate southeast storm waves ($H < 0.6$ m; $T > 8$ s) may promote building at any of the beaches. Fair-weather southwest waves generally cause accretion but when wave conditions of $H > 1$ m and $T < 6$ s are present the beaches may also erode.

8. An early September nearshore survey does not show offshore bars. The absence of these bars may indicate stored offshore sand has been moved onshore which is compatible with general building conditions of the beaches observed at that time.

LITERATURE CITED

Anonymous. 1963. Rhode Island, Block Island Sound, Ninigret Pond to Nebraska Shoal. Hydrographic Survey No. 8615, U.S. Coast and Geodetic Survey.

Anonymous. 1961. Rhode Island, Block Island Sound, Ninigret Pond East. Hydrographic Survey No. 8616, U.S. Coast and Geodetic Survey.

Anonymous. 1970. Summary of Synoptic Meteorological Observations, North American Coastal Marine Area. U.S. Naval Weather Service.

Anonymous. 1971. Block Island Sound and eastern Long Island Sound - tide current chart. National Ocean Survey, U.S. Dept. of Commerce, 29 p.

Anonymous. 1975. Charlestown Hydrographic Study, April 1974 to April 1975. Raytheon Company, Final Report.

Anonymous. 1976. Tide tables: high and low water predictions East Coast of North and South America, including Greenland. National Ocean Survey, U.S. Dept. of Commerce, 288 p.

Bagnold, R. A. 1963. Beach and nearshore processes, Part 1. Mechanics of marine sedimentation. In The Sea, M. N. Hill (ed.), Volume 3, p. 507.

Bagnold, R. A. 1966. An approach to the sediment transport problem from general physics. U.S. Geol. Surv. Prof. Pap. 422-I, 37 p.

Bascom, W. 1964. Waves and beaches: the dynamics of the ocean surface. Doubleday and Co., Inc., New York, 267 p.

Beale, R. 1975. Beach-nearshore sediment distribution and its relationship to beach processes, Matunuck Beach, Rhode Island.

Master's Thesis (Unpub.), University of Rhode Island, Kingston, Rhode Island.

Bretschneider, C. L. 1952. Revised wave forecasting relationships. Proc. of the Second Conf. on Coastal Engineering.

Bryant, Edward A. 1974. A comparison of air photograph and computer simulated wave refraction patterns in the nearshore area, Richibucto, Canada and Jervis Bay, Australia. Maritime Sediments, 10(3): 85.

Bumpus, D. F., R. E. Lynde and D. M. Shaw. 1972. Physical oceanography. In Coastal and Offshore Environmental Inventory. Cape Hatteras to Nantucket Shoals. Complimentary Volume. Marine Experiment Station, Graduate School of Oceanography, University of Rhode Island Occasional Pub. No. 6.

Corps of Engineers. 1950. South shore, State of Rhode Island, beach erosion control study. Army Corps of Engineers, 81st Congress House Document No. 490. Government Printing Office, Washington, D.C.

Dillon, W. P. 1970. Submergence effects on a Rhode Island barrier and lagoon and inferences on migration of barriers. Jour. Geol., 78(1): 94-106.

Dobson, R. S. 1967. Some applications of a digital computer to hydraulic engineering problems. Dept. of Civil Engineering, Stanford University, Stanford, California, Tech. Rept. No. 80.

Havens, J. M., D. M. Shaw and E. R. Levine. 1972. Offshore weather and climate. In Coastal and Offshore Environmental Inventory. Cape Hatteras to Nantucket Shoals. Complimentary Volume. Marine Experiment Station, Graduate School of Oceanography, University of

Rhode Island Occasional Pub. No. 6.

Inman, D. L. 1960. Shore processes. In McGraw-Hill Encyclopedia of Science and Technology, v. 12, McGraw-Hill, p. 299-306.

Inman, D. L. and R. A. Bagnold. 1963. Littoral processes. In The Sea, v. 3, M. N. Hill (ed.), Interscience.

Kelley, T. A. 1960. Plane Surveying, Field Manual. Colorado School of Mines, Golden, Colorado, 229 p.

Komar, P. D. 1974. Nearshore currents and sediment transport, and the resulting beach configuration. In The New Concepts of Continental Margin Sedimentation, I-VI. Am. Geo. Inst., Short Course Lecture Notes, p. 431-467.

Kramer, W. P. and R. H. Weisberg. 1975. Fortran graphics programs for physical oceanographic and time series data. Sea Grant, University of Rhode Island Marine Tech. Report 46.

McMaster, R. L. 1960. Mineralogy as an indicator of beach sand movement along the Rhode Island shore. Jour. of Sed. Pet. 30(3): 404-413.

McMaster, R. L. 1961. Transit surveys of selected Block Island Sound beaches in Washington County, Rhode Island, 1964-1975, v. 1-5. University of Rhode Island, Kingston, Rhode Island.

May, J. B. and W. Tanner. 1973. The littoral power gradient and shoreline changes. In Coastal Geomorphology, Coates (ed.), p. 43-60.

Nichols, R. L. and A. F. Marston. 1939. Shoreline changes in Rhode Island produced by the 1938 hurricane. GSA, 50: 1357-1370.

Pierson, W. J., Jr., G. Neumann and R. W. James. 1955. Practical methods for observing and forecasting waves by means of wave spectra and statistics. H.O. Publ. 603, U.S. Navy Hydrographic Office.

Shepard, F. P. and D. L. Inman. 1950. Nearshore circulation related to bottom topography and wave refraction. Am. Geophys. Union Trans., 31: 196-212.

Sverdrup, H. V. and W. H. Munk. 1947. Wind, sea and swell: theory of relations for forecasting. H.O. Publ. No. 601, U.S. Navy Hydrographic Office.

Swift, D. J. P. 1976. Coastal sedimentation. In Marine Sediment Transport and Environmental Management, D. J. Stanley and D. J. P. Swift (eds.), Chpt. 14, John Wiley and Sons, N.Y., p. 255-

Tanner, W. F. 1976. Effects of Hurricane Eloise on beach and coastal structures, Florida Panhandle: Comment and reply. Geology 4(10): 633-634.

Wilson, W. S. 1966. A method for calculating and plotting surface wave rays. Tech. Mem. No. 17, U.S. Army Corps of Coastal Eng. Res. Ctr., p. 57.

APPENDIX A

PROCEDURES AND METHODS

Profiles

The profiles were determined by a standard technique of hand leveling and slope chaining (Kelly, 1960). The leveling was employed to obtain the elevation of the points with respect to the reference point. It was accomplished by planting two marked, pointed, seven foot rods at the breaks in slope and backsighting and foresighting on the rods. A 100 foot tape measure was then used to measure the slope distance between the poles. This procedure was carried out on all beaches from the reference point to the waterline. On two occassions the wind did not permit easy use of the tape measure so pacing was employed. Only once was the wind such that the rods were unusable and on that occassion the dip meter of the Brunton was pressed into service. While the Brunton and pace method does not give the accuracy of the leveling method, it did provide an estimate of the profiles. The profiles were plotted on the same scale as those from the McMaster (1961) survey for comparison.

Wave Observations

The angle of wave approach was obtained by determining the bearing of the perpendicular to the wave fronts with a Brunton compass (Pierson et al., 1955). Observations from the middle of the beach face provided the best vantage point for the sightings. However, there were times when a reliable direction was difficult to determine, particularly at Weekapaug, and several attempts had to be made.

Timing the waves as they broke with a stopwatch provided a measure

of the periodicity of the waves (Pierson et al., 1955: modified). It was common to time ten waves and if the period of the individual was sufficiently close to the others the average was recorded as the period. This would be more properly called the significant period. There were several occassions when 50 waves had to be times to provide a reasonable estimate. This was particularly true when storm seas and decaying swells were entering the Sound. Also, the percentage of the wave periods was estimated, especially when storm seas or decaying swells were present.

The height determinations were obtained by comparing the breakers just before they break to one of the level rods, while standing near the waterline. Ten waves were used to get an accurate estimate. As before, percentages of wave heights were estimated and correlated with the wave periods.

Longshore Drift

A piece of wood was thrown into the surf and timed over a distance of 30 feet to ascertain the longshore drift (Bascom, 1964). When the surf was extremely heavy, this was not done because it was impossible to see the object floating in the foam.

Nearshore Topography

Nearshore soundings were made by using a procedure modified from a method proposed by Bascom (1964). A Raytheon DE 725-C fathometer interfaced with a UHER 4400 stereo tape recorder (LeBlanc, pers. comm.)

was employed, since the paper record produced by the fathometer, was inadequate for interpretation. The recorded signals were digitized and then programmed through the Ocean Engineer's Nova computer (Milligan, pers. comm.). The printout was expanded so that the output could be conveniently analyzed. The strip recording given by the fathometer was used for monitoring purposes.

Wind Data

The Coast Guard at Point Judith and the New England Electric Company from their Charlestown recording tower provided wind data for the study period. This was part of the effort to monitor the local wind patterns and determine their influence on the wave patterns. In order to be able to compare the two sets of data, a three point running average of the Charlestown data had to be made. These data were then plotted on rosette diagrams (Corps of Engineers, 1950) and compared.

Hindcasting

In order to get a complete picture of the wave energy in Rhode Island Sound, the height and direction of the swells entering the Sound were determined. To do this, six-hour synoptic weather maps were obtained from the Geography Department (Havens, pers. comm.) and the Sverdrup-Munk-Bretschneider hindcasting method (1952) was used. This method only gives significant height and period, unlike the Pierson, Neumann and James co-cumulative method (1955). However, the SMB method was sufficient because the beach observer could only record the significant height and period.

Computer Model

All the foregoing methods were intended either to provide input information or comparison for the May and Tanner model (1973) computer program. The program is designed to calculate coastal energy given the bathymetry and deepwater wave characteristics. The program had to be adapted to the IBM 360 system because it was developed on a CDC system. This required all the original plot routines to be discarded. In place of the discarded plot routines the LINLIN plot program (Kramer et al., 1974) was substituted. For more detailed plots close to shore, two more plot programs were written. The first program was designed to write down the nearshore depths of the three beaches from cards. Each plot was hand contoured. The second was written to search through the generated wave ray file and plot the nearshore portion of the rays. Both programs were produced on the same scale, so the rays could be overlaid on the appropriate bathymetry.

Hydrographic boatsheets (8615, 8616) were used for the bathymetry. They were first contoured and then a grid was overlaid on the maps. The grid was marked in unit squares of 1 cm by 1 cm (100 m X 100 m) to insure the proper detail of topography.

When all the development and digitizing were finished, the program and data set were stored in files on the computer for each accessing.

When a run was desired the wave data from the field data, weather maps, Dr. Oviatt's (pers. comm.) Point Judith study, or Meterological Synoptic data was used and the program would produce the results. If the run was one of value, the rays and shoreline were plotted for an overall picture.

APPENDIX B

BEACH RESPONSE STYLE AND BREAKER ENERGY

Initially it was believed that plotting the May and Tanner (1973) littoral component of wave power (P_L) for the coastline would be ineffective in resolving the question as to why the individual beaches tended to respond independently of one another under a given set of wave conditions. Instead, it was thought that the question could best be explained by analyzing the amount and variation of wave energy impinging upon the beaches. The approach appeared to be of value since the breaker power was the basis for the longshore power,

$$P_L = 0.5\ P_b \sin(2\beta)$$

Thus the breaker power was expected to give appropriate information for establishing a relationship. In the analyses two wave regimes were introduced to the May and Tanner (1973) computer program. These were chosen because the wave characteristics were the same on all three beaches and provided two different approach directions. The output included shoreline breaker position, breaker energies, and the position of energy peaks in reference to protruberances along the shoreline.

The breaker energy were plotted against breaker positions for the wave regime, 180°T, H = 0.4m, T = 4s (Fig. 15). In this case the energy peaks were to the west of the prominent shoreline projections. By summing the area under the curves the total energy was determined and the highest value was attained for East Beach (Table 8). However, the lengths of the breaker coordinate axes were not equal for the beaches, so mean energy values were computed. For the given wave condition the highest mean value did not correspond to East Beach, the positive responding beach, but to Green Hill.

Figure 15. Plots of breaker energy ($g \cdot cm/s^3$) computed by the May and Tanner (1973) model against the position of the breaker on the shoreline (0.1 km) for $180^{\circ}T$, T=4 s, H=0.46 m. The three plots are for Weekapaug (W), East Beach (E), and Green Hill (G) with appropriate shorelines displayed.

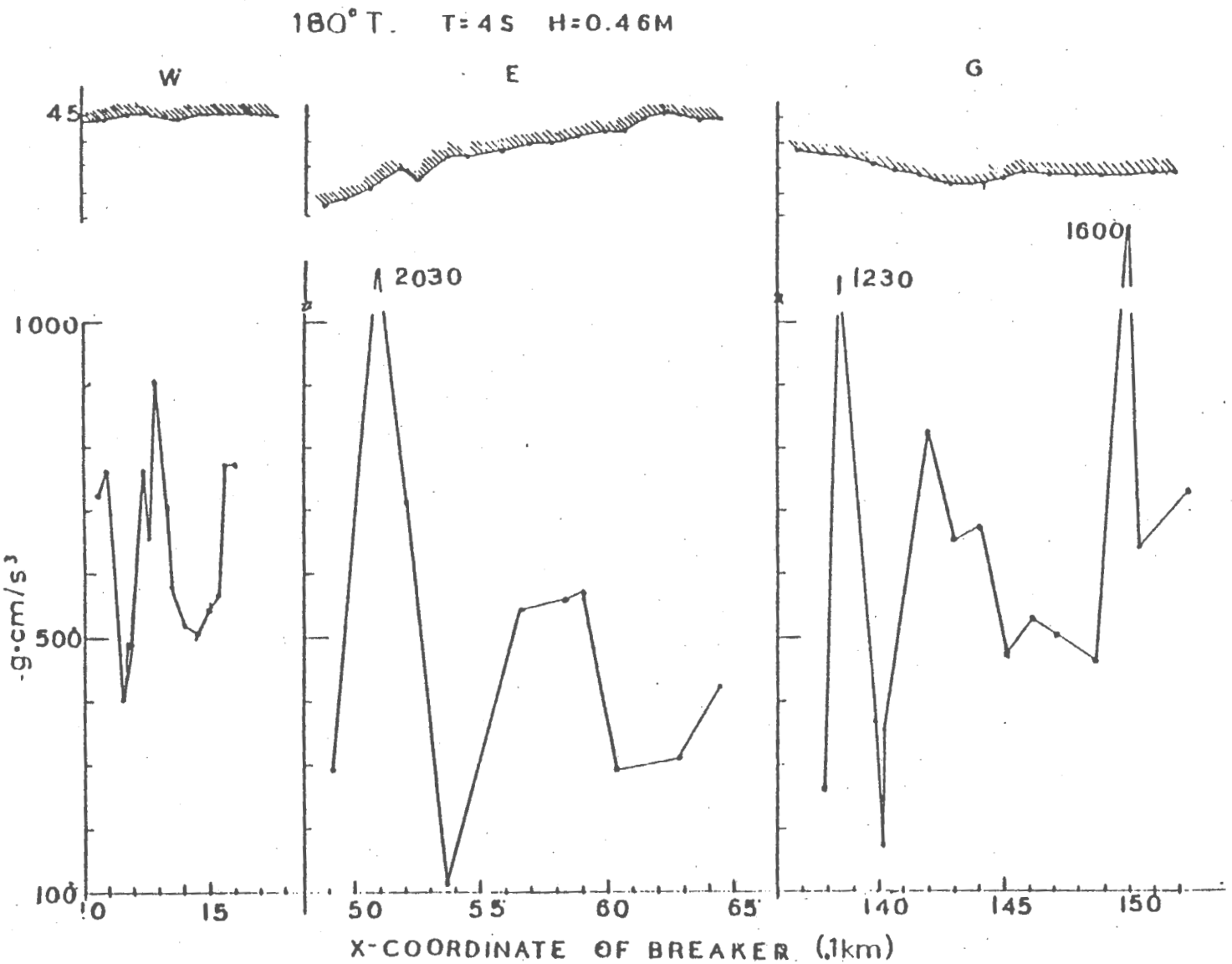
180° T. T=4S H=0.46M
W
E
G
45
2030
1230
1600
1000
500
100
-g·cm/s³
10
15
50
55
60
65
140
145
150
X-COORDINATE OF BREAKER (1km)

Table 8. Breaker Energy

	Total Energy ($g.cm/s^3$) ($\times 10^8$)	Mean Energy ($g.cm/s^3.cm$) ($\times 10^3$)
Angle = 180° T		
Weekapaug	3.46	6.40
East	9.24	6.10
Green Hill	8.96	6.63
Angle = 200° T		
Weekapaug	2.94	2.83
East	3.78	2.41
Green Hill	3.53	2.86

Bartlett's test for the homogeneity of variance was then employed to determine if the variance in energy was responsible for the response styles. For this case the underlying variability in the energy was significantly greater for East Beach and Green Hill than for Weekapaug. Therefore, more erosion or deposition would be expected at East and Green Hill under the wave regime, 180°T, H = 0.4m, T = 4s.

The other wave regime analyzed was 200°T, H = 0.3m, T = 5s (Fig. 16). In this example the energy peaks were to the east of the prominent shoreline projection. Although the highest total energy was at East Beach, the highest mean energy occurred at Green Hill (Table 8). Bartlett's test showed none of the variances differed significantly. Thus, deposition or erosion would not be expected to be significantly different from beach to beach. The analysis was abandoned because no correlation between total energy and response styles or variance of energy and response styles could be found.

Figure 16. Plots of breaker energy ($g \cdot cm/s^3$) computed by the May and Tanner (1973) model against the position of the breaker on the shoreline (0.1 km) for $200^{o}T$, T=5 s, H=0.37 m. The three plots are for Weekapaug (W), East Beach (E), and Green Hill (G) with appropriate shorelines displayed.

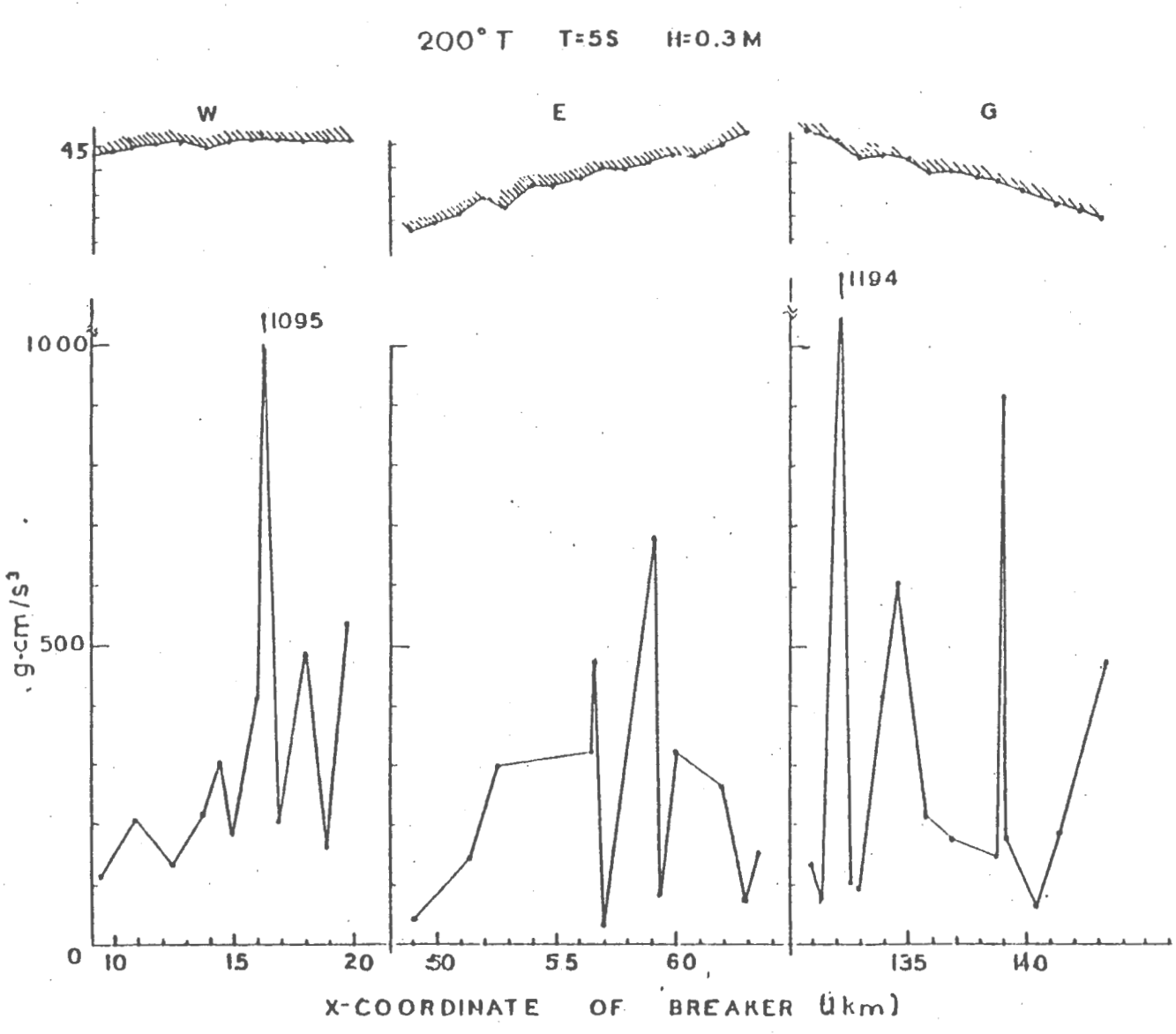
200° T T=5S H=0.3 M
W
E
G
45
1095
1194
1000
500
0
g-cm/s³
10
15
20
50
55
60
135
140
X-COORDINATE OF BREAKER (km)

APPENDIX C

FAIR-WEATHER AND STORM WAVE RESPONSE PREDICTION

A method for predicting beach change trends based upon long range weather forecasts was attempted by reproducing fair-weather-storm depositional and erosional cycles observed on the beaches during the years of surveying. A successful test would permit this method to be used for prediction of beach change trends based upon long range weather forecasts. The procedure called for a definition of representative fair-weather and storm wave regimes so that characteristic May and Tanner (1973) longshore power (P_L) and associated accretion-erosion potential curves (ΔP_L) could be developed. Sets of wave conditions were selected from Table 5. These data were weighted for fair-weather and storm conditions according to field observations and SSMO wind and wave compilations (Anonymous, 1970). An equation was written in the following general form

$$\sum_{i=1}^{n} \alpha_i (A,P,H)_i \text{ , and } \sum_{i=1}^{n} \alpha_i = 1 \qquad (3)$$

where α_i = weighting proportion, A = wave approach angle (°T), P = wave period (s), H = wave height (m), and n = number of wave types selected. The parenthetical expression represents the P_L for that set of wave conditions. The specific computation for the fair-weather condition was

$$0.45(200,4,0.1) + 0.32(180,4,0.1) + 0.07(160,4,0.1) + 0.16(140,4,0.1) \qquad (4)$$

using these wave characteristics, P_L and ΔP_L values were computed and plotted. A comparison between the fair-weather ΔP_L curve and the summed beach surveys revealed no agreement relative to net erosional-

accretional conditions. A second trial was made, but this time the period was changed from 4s to 6s. Although some conformity was achieved, no significant correlation resulted.

For storm conditions, the computation was

$$0.60(200,4,0.1) + 0.13(180,6,0.1) + 4.0(160,4,1.5) + 0.11(140,9,0.1) + 0.11(120,9,0.1) \quad (5)$$

where α_3 (4.0) was multiplied by 100, because the energy associated with 1.5 m is about 100 times greater than that related to 0.1 m. The P_L and ΔP_L curves were computed and plotted as before. The comparison between the storm ΔP_L curve and the summed winter surveys indicated there was no correlation.

Thus the attempt to predict fair-weather and storm wave responses in terms of seasonal beach accretional-erosional cycles was abandoned. Since the fair-weather wave average should have closely approximated the day-to-day wave regimes, better agreement was expected, but it was not achieved due to the fact that those important energy spikes associated with storms were diluted as a result of the low probability of storm occurrences and not enough wave regimes were considered. On the other hand, as a consequence of this averaging process, the mean storm wave condition minimized the effect of storm pulses, while the storm surveys maximized their effect, thus resulting in a poor correlation.

APPENDIX D

WAVE ATTENUATION

The May-Tanner computer model (1973), as with similar computer models, must have as input data, starting coordinates for the wave rays. All the wave rays in this investigation initially were evenly spaced in the shore parallel direction. For this portion of the study the original spacing of 0.1 km proved to be too coarse as the energy peaks (Appendix B) appeared to be isolated and erratic. To determine if the peaks were real, the spacing of the wave rays was reduced to 10 m and 50 m. With these spacings the peaks proved to be real and a result of refraction. The control the bathymetry exerted on the wave-ray paths was well-illustrated in Figure 17. This figure indicated the bathymetric control of wave refraction in the whole study area. In some of the figures wave rays showed diverging patterns as a result of shoal areas such as Nebraska Shoals or off Quonochontaug Point (Fig. 17). Other plots showed wave rays stopping before they reached the shore due to abrupt bathymetric changes and shoal areas (Fig. 17). These areas caused the rays to meet breaking criteria before encountering the shore. The diverging patterns indicated zones of energy concentration and hence potential areas of erosion for waves of similar characteristics. The abrupt stopping wave rays designated areas where waves of similar characteristics might be expected to undergo attenuation. This in turn would define areas along the coast that would be more sheltered from various wave regimes as a result of attenuation for waves approximating the same conditions.

Figure 17. Computer display of wave rays approaching from 200°T, T=5 s, H=0.3 m impinging on all three beaches. The grid system for the program is shown and the scale is 10 units =1 km.

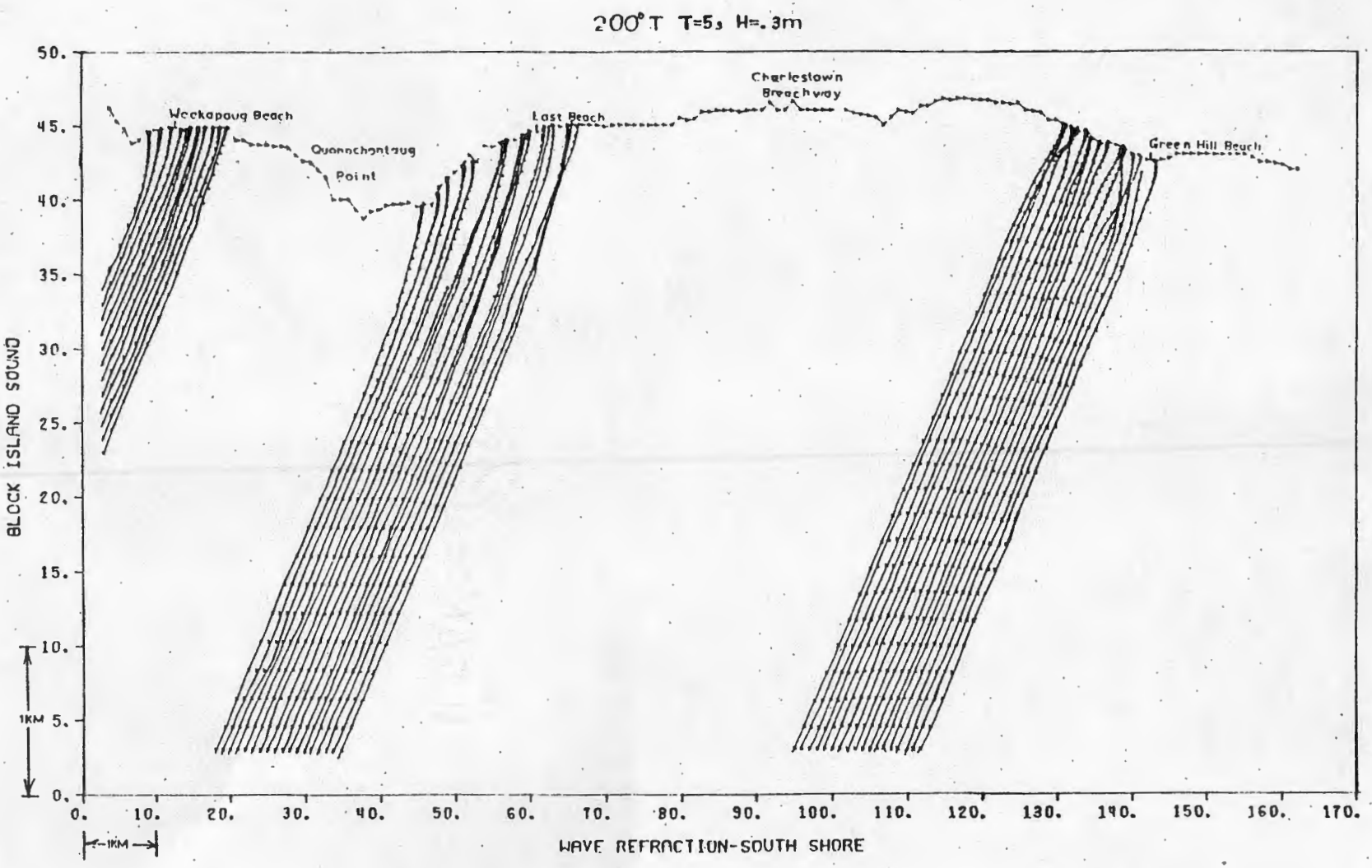
200° T T=5s H=.3m
Weekapaug Beach
Quonnchontaug
Point
East Beach
Charlestown
Breachway
Green Hill Beach
BLOCK ISLAND SOUND
50.
45.
40.
35.
30.
25.
20.
15.
10.
5.
0.
1KM
0.
10.
20.
30.
40.
50.
60.
70.
80.
90.
100.
110.
120.
130.
140.
150.
160.
170.
1KM
WAVE REFRACTION-SOUTH SHORE

APPENDIX E

CORRELATION OF ANGLE β AND LONGSHORE COMPONENT OF WAVE POWER

The longshore drift has already been shown to be a function of the angle β. After the graphs of the angles with all possible height and period combinations were made, a question was raised as to how the β angle interacted with the period and height of given wave conditions.

A brief effort was made to determine whether a simple relationship existed between the approach and β angles. If successful an insight could be gained into the specific influence the approach angle has on the longshore component of wave power. However, as a result of mathematical complications related to wave refraction, the solution was complex and iterative and was not attempted.

Next an attempt was made to determine the association between the angle β and the longshore component of wave power. To accomplish this, the power equation was resolved into its basic components such as height and period, and P_L was given an arbitrary energy value of 20 X 10^5 g · cm/s^3 which was based upon the bracketing value from the angle with all possible height and period combination graphs. Also, while the power expression was in its basic form, the relationship between height and period was evaluated.

The longshore power equation, P_L, in basic components was:

$$P_L = \{\tfrac{1}{2}[H^2 aT \tanh(bD/T^2)] + [(cD/aT \tanh(bD/T^2))$$
$$T/\sinh(2cD/aT^2 \tanh(bD/T^2))] [H^2 aT \tanh(bD/T^2)]\}$$
$$\{\tfrac{1}{2}\sin(2\beta)\}1256$$

where a = 1.56, b = 4.0256, c = 6.28, D = 0.3m, H = wave height (m), T = wave period (s), and 1256 = a conversion factor. This is usually written as the power equation multiplied by $(\tfrac{1}{2}\sin(2\beta))$.

To force P_L to 20 X 10^5 g · cm/s^3, a set of height and periods were used with a variety of β angles (Table 9). Generally, as the angle β became smaller, shorter periods were required to bring the larger heights down to 20 X 10^5 g · cm/s^3 (Table 10). However, as the β angles closely approached 45°, the period at a given height levelled off and began to decrease. This was judged to be an effect of the hyperbolic trigonometric functions (Table 10).

The evaluation of the relationship of height and period in the longshore power equation established height as the dominant factor. In the first expression, $[\frac{1}{2}(H^2aT \tanh(bD/T^2)]$, of the power equation the height which is squared controlled the term and in turn contributes most to the computations. For this expression when only the height was increased, the calculations increased an order of magnitude (Table 11). However, when only the period was increased, the computations changed much less than an order of magnitude. To reiterate then, this term was the most influential in the total equation and was greatly increased by larger values of height.

The second expression, $[\frac{cD/(aT \tanh(bD/T^2))T}{\sinh(2cD/aT^2 \tanh(bD/T^2)}][H^2aT \tanh(bD/T^2)]$, was influenced most by the period. When only the period was increased, the calculation decreased an order of magnitude for every second of period increase. When the height was increased, the computation also increased an order of magnitude because of the second part of the expression $(H^2aT \tanh(bD/T^2))$. Finally, when combined with the first expression, the second merely modified the total result (Table 11).

Table 9. Angles, heights, and periods used in correlating angle β and P_L

β (^{o})	Height Ht (m)	Period T (s)
1¼	0.5	2.
2½	1.0	4.
5	1.5	6.
10	2.0	8.
20		
30		

β, Ht, and T were used in all possible combinations (96).

Table 10. Distribution of β, Height, and Period Giving a Stated P_L^*

β (°)													
1¼		2½		5		10		20		30		40	
Ht(m)	T(s)	Ht(m)	T(s)	Ht(m)	T(s)	Ht(m)	T(s)	Ht(m)	T(s)	Ht(m)	T(s)	Ht(m)	T(s)
0.5	<1	0.5	1	0.5	3	0.5	5	0.5	7	0.5	7	0.5	3
1.0	3	1.0	5	1.0	9								
1.5	6	1.5	>10										
2.0	8												

* $P_L = 20 \times 10^5$ g.cm/s^3

Table 11. Component Values for Power Equation

Height (m)	Period (s)			
	2	4	6	8
0.3:				
HATANH	0.4115 E-011	0.2115 E-01	0.1412 E-01	0.1059 E-01
STANH	0.5506 E-02	0.1120 E-03	0.2074 E-05	0.3808 E-07
TOTAL	0.1499 E-01	0.6835 E-02	0.4540 E-02	0.3406 E-02
0.5:				
HATANH	0.1143 E+00	0.5876 E-01	0.3923 E-01	0.2943 E-01
STANH	0.1529 E-01	0.3112 E-03	0.5761 E-05	0.1058 E-06
TOTAL	0.4165 E-01	0.1899 E-01	0.1261 E-01	0.9460 E-02
1.0:				
HATANH	0.4572 E+00	0.2351 E+00	0.1569 E+00	0.1177 E+00
STANH	0.6117 E-01	0.1245 E-02	0.2304 E-04	0.4231 E-06
TOTAL	0.1666 E+00	0.7594 E-01	0.5045 E-01	0.3784 E-01
1.5:				
HATANH	0.1029 E+01	0.5289 E+00	0.3531 E+00	0.2649 E+00
STANH	0.1376 E+00	0.2801 E-02	0.5186 E-04	0.9520 E-06
TOTAL	0.3748 E+00	0.1709 E+00	0.1135 E+00	0.8514 E-01
2.0:				
HATANH	0.1829 E+01	0.9402 E+00	0.6278 E+00	0.4709 E+00
STANH	0.2447 E+00	0.4979 E-02	0.9218 E-04	0.1692 E-05
TOTAL	0.6664 E+00	0.3038 E+00	0.2180 E+00	0.1514 E+00

$\beta = 10^{o}$; HATANH = $\frac{1}{2}\{H^2 aT \tanh(bD/T^2)\}$; TOTAL = HATANH + STANH $\{\frac{1}{2}\sin(2\beta)\}$;
STANH = $\{(cD/(aT \tanh(bD/T^2)))\sinh(2cD/(aT^2 \tanh(bD/T^2)))\}\{H^2 aT \tanh(bD/T^2)\}$.

Thus, this term with the hyperbolic functions did increase with the period, but added very little to the total.

In summary, as the β angle decreased and the heights increased, successively shorter periods were required to force equation (6) to 20×10^5 g · cm/s^3. This indicates that sin(2β) had an important influence on the value of P_L. Coupled with the period it was able to reduce the effect of the height. However, as shown above height was more important than period in determining the power. This ability of the period to limit the influence of the height is related to the hyperbolic geometric function as illustrated previously.

APPENDIX F

NUMERICAL COMPARISON OF PROFILES AND THE POTENTIAL EROSION-ACCRETION CURVES

A rough set of calculations undertaken to determine if the May and Tanner (1973) model could account approximately for the volume of sand the selected beach surveys indicated was moved. Two surveys at Weekapaug, January 10 and January 17, 1975, were selected for comparison. The profiles for the two dates were plotted to obtain the amount of sand lost or gained. For width a meter was chosen because wave power was resolved in terms of a meter distance along a wave crest. The volume was then divided into simple geometric solids for easy computation (Fig. 18).

The volume of a prism was given by:

$$\begin{aligned} V &= \tfrac{1}{2}bhd \\ &= \tfrac{1}{2}\ (1.82)(0.15)(1.0) \\ &= 0.14\ m^3\ , \end{aligned} \qquad (7)$$

while the volume of a parallelpiped was:

$$\begin{aligned} V &= bhd \\ &= (10.91)(0.15)(1.0) \\ &= 1.65\ m^3\ . \end{aligned} \qquad (8)$$

Therefore the total volume was 1.79 m^3 or 1.78 X 10^6 cc. For January 10 the measure P_L (May and Tanner, 1973) from the wave regime os 140°T, H = 0.1m, T = 6s was -8 X 10^5 g · cm/s^3 (negative sign denotes deposition). This value was converted into sand transport rate, q, by:

$$q = kP_L/(\rho_s - \rho)ga \qquad (9)$$

where P_L = littoral component of wave power, ρ_s = density of the sand

Figure 18. (a) The geometric representation of the volume transported at Weekapaug between January 10 and 17.

(b) Prism part of decomposed volume.

(c) Parallelpiped part of decomposed volume.

a

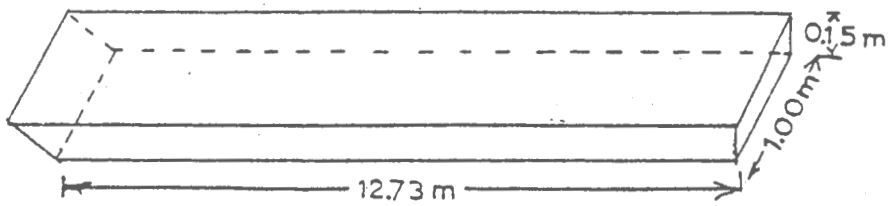

b

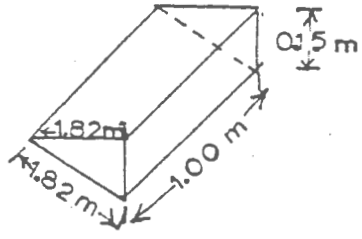

c

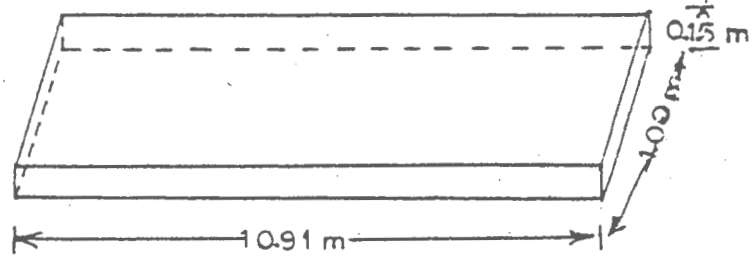

(2.6 g/cc), g = gravitational acceleration, a = pore space factor (0.6), k = dimensionless coefficient which has the "instantaneous" value of 0.77 (Komar and Inman, 1970). Thus,

$$q = \frac{0.77\ (-8 \times 10^5\ g \cdot cm/s^3)}{(2.6\ g/cc - 1.0\ g/cc)(980\ cm/s^2)(0.6)}$$

$$= -6.55 \times 10^2\ cc/s \quad .$$

Assuming the waves came from the southeast for 84 hours or 3.02×10^5 s, the total amount of sand transported, Q, was calculated as

$$Q = q \cdot time$$

$$= -6.55 \times 10^2\ cc/s\ (3.02 \times 10^5\ s) \qquad (10)$$

$$= -1.98 \times 10^8\ cc \quad .$$

For January 17, 1975 the wave regime was 200°T, H = 0.1m, T = 4s, and the associated $P_L = 4.6 \times 10^5\ g \cdot cm/s^3$. Using the same equations above, q was 4.91×10^2 cc/s. The waves were assumed to have come from 200°T for 72 hours or 2.59×10^5 s. Q was then found to be

$$Q = 4.91 \times 10^2\ cc/s\ (2.59 \times 10^5\ s)$$

$$= 1.27 \times 10^8\ cc \quad .$$

The total amount of sand moved according to the May-Tanner model was the sum of the above two results,

$$-1.98 \times 10^8\ cc + 1.27 \times 10^8\ cc = -7.1 \times 10^7\ cc\ (deposition).$$

According to the profiles the total volume of sand accreted was 1.78×10^6 cc, while the May-Tanner model predicted the deposition of

7.1×10^7 cc of sand. Thus the values differed by an order of magnitude. However, this result, although significant, does not negate the usefulness of the exercise. Previously it was unknown as to what extent the model was capable of predicting the sand volume changes. The fact that the difference was less than 5, 10 or more orders of magnitude was profitable, because the size of the error is not recognized.

APPENDIX G

BEACH SURVEYS, P_L AND ΔP_L CURVES

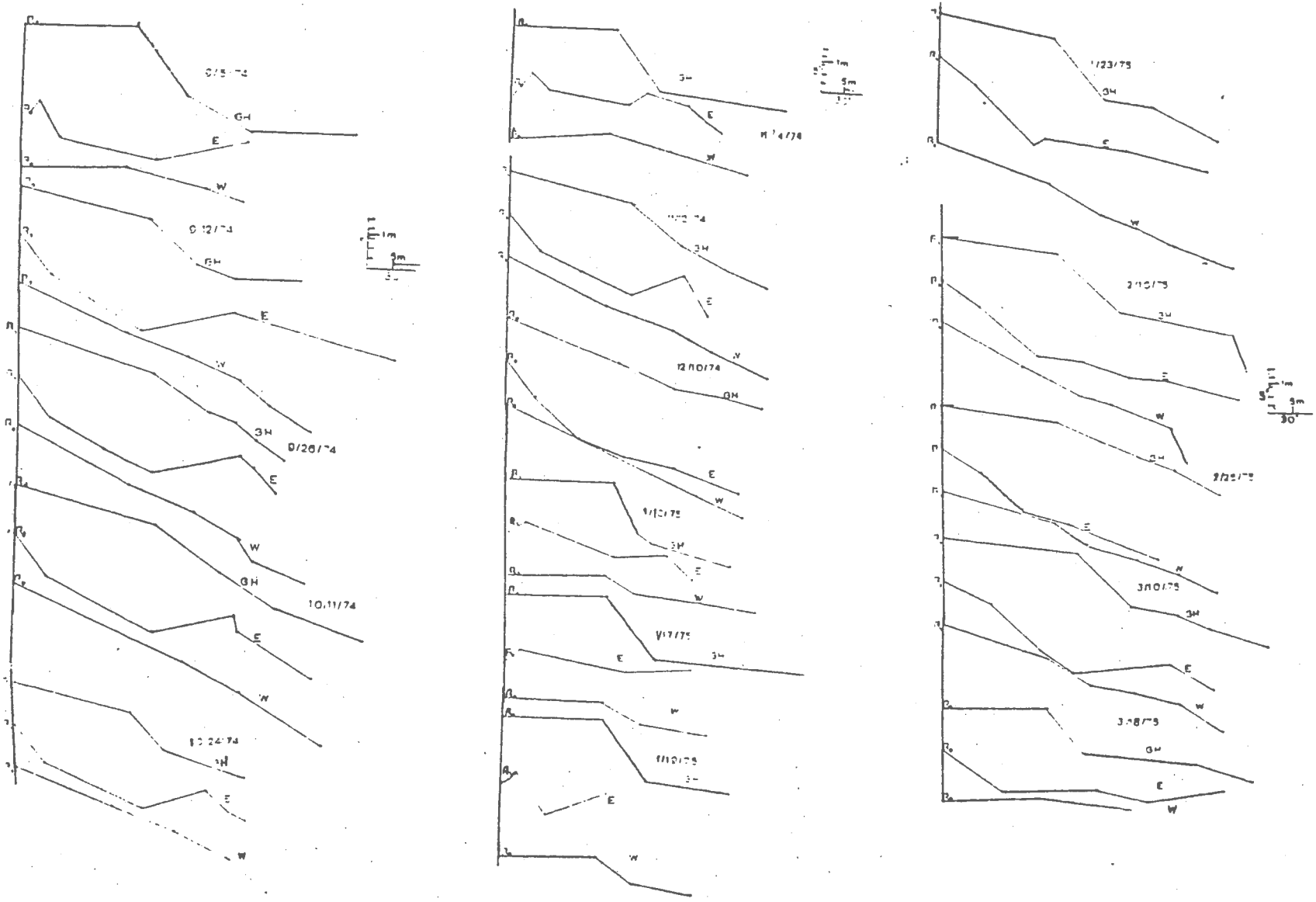
GH
E
W
GH
E
W
3H
E
W
GH
E
W
GH
E
W
3H
E
W
3H
E
W
GH
E
W
3H
E
W
3H
E
W
GH
E
W

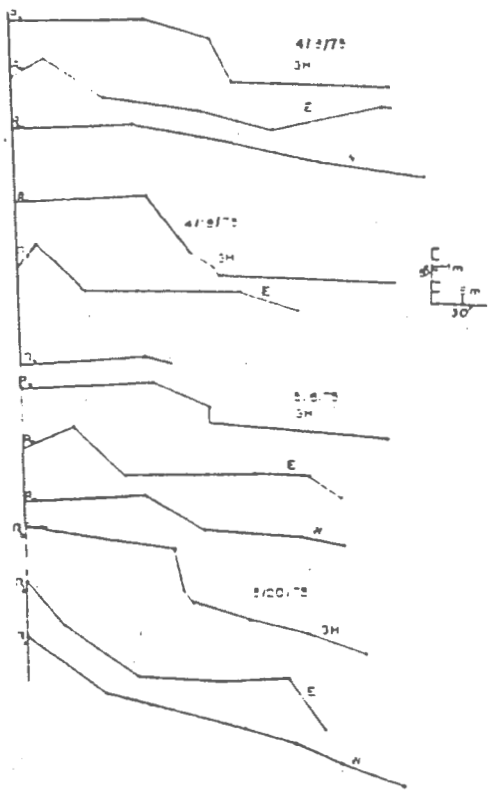
3M
E
W
3M
E
3M
E
W
3M
E
N

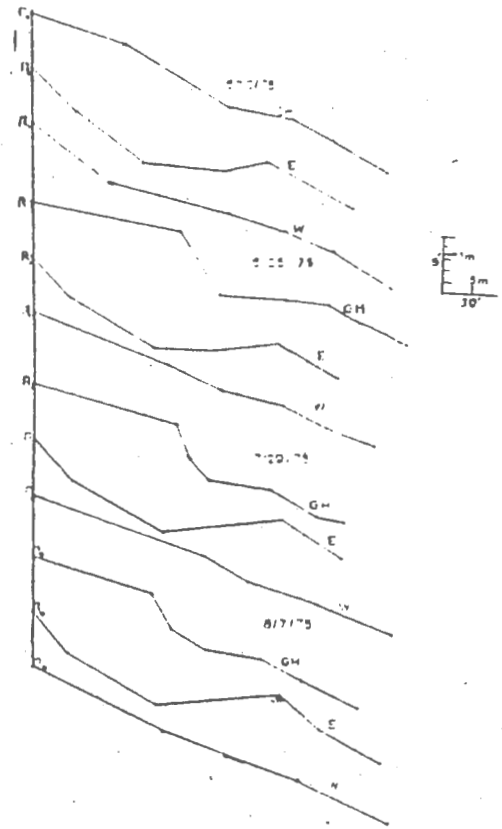
E
W
GH
E
GH
E
GH
E

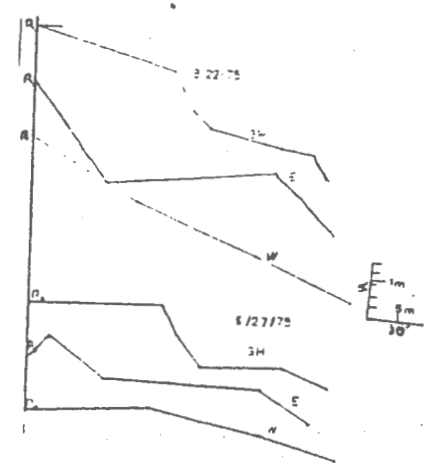
3M
E
W
3M
E
N

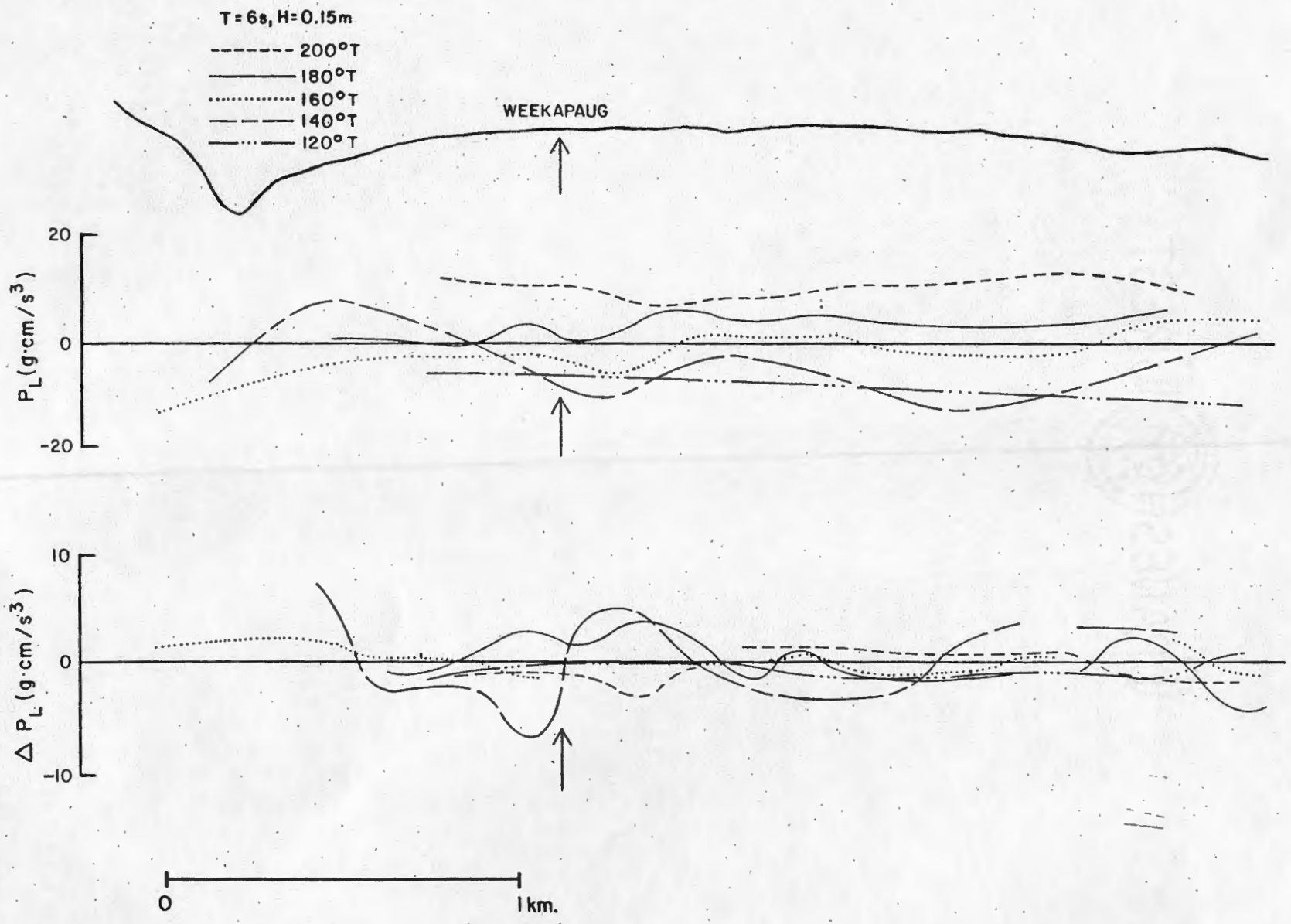
T = 6s, H = 0.15m
200°T
180°T
160°T
140°T
120°T
WEEKAPAUG
20
0
-20
P_L (g·cm/s^3)
10
0
-10
ΔP_L (g·cm/s^3)
0
1 km.

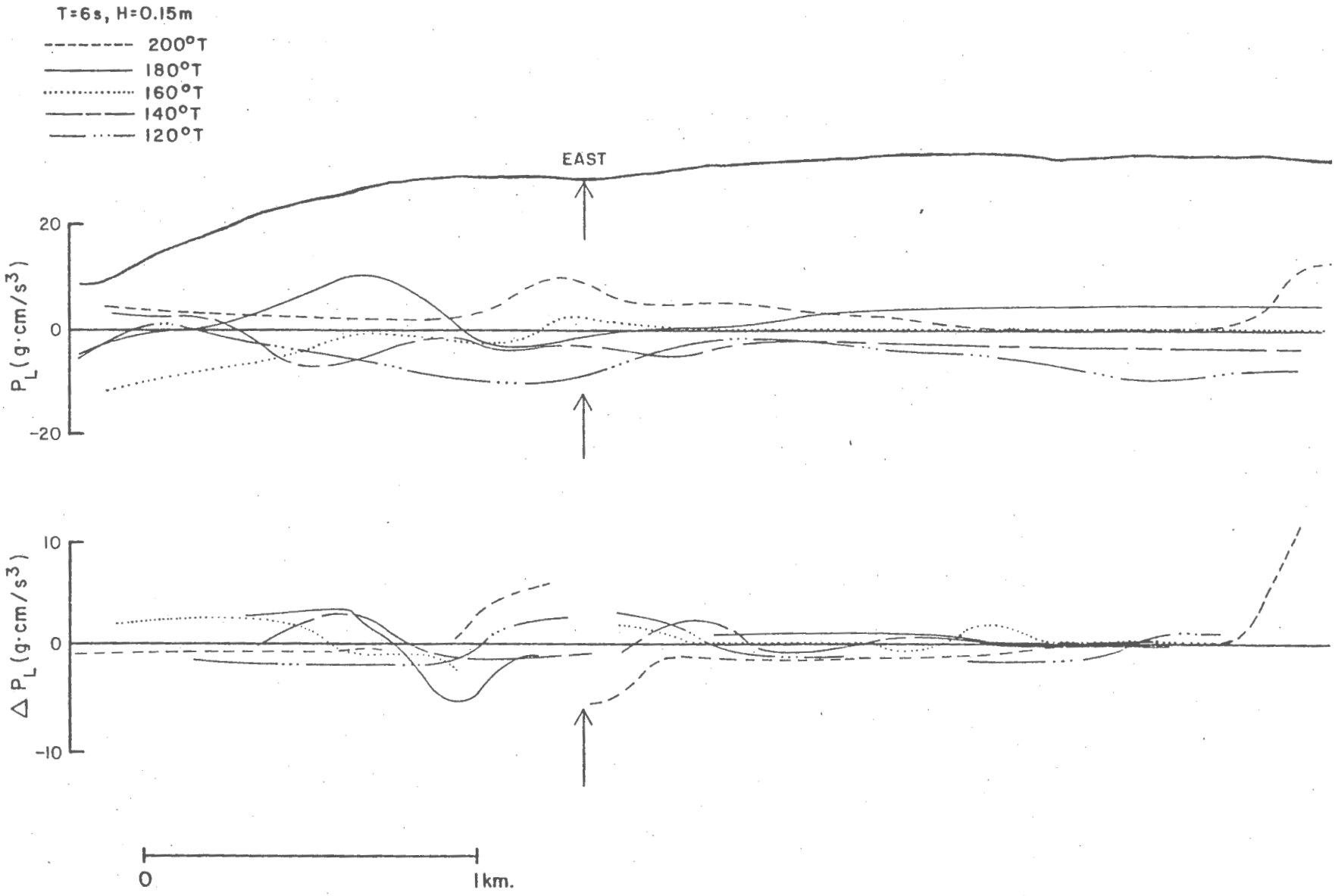
T=6s, H=0.15m
200°T
180°T
160°T
140°T
120°T
EAST
20
0
-20
P_L (g·cm/s^3)
10
0
-10
ΔP_L (g·cm/s^3)
0
1km.

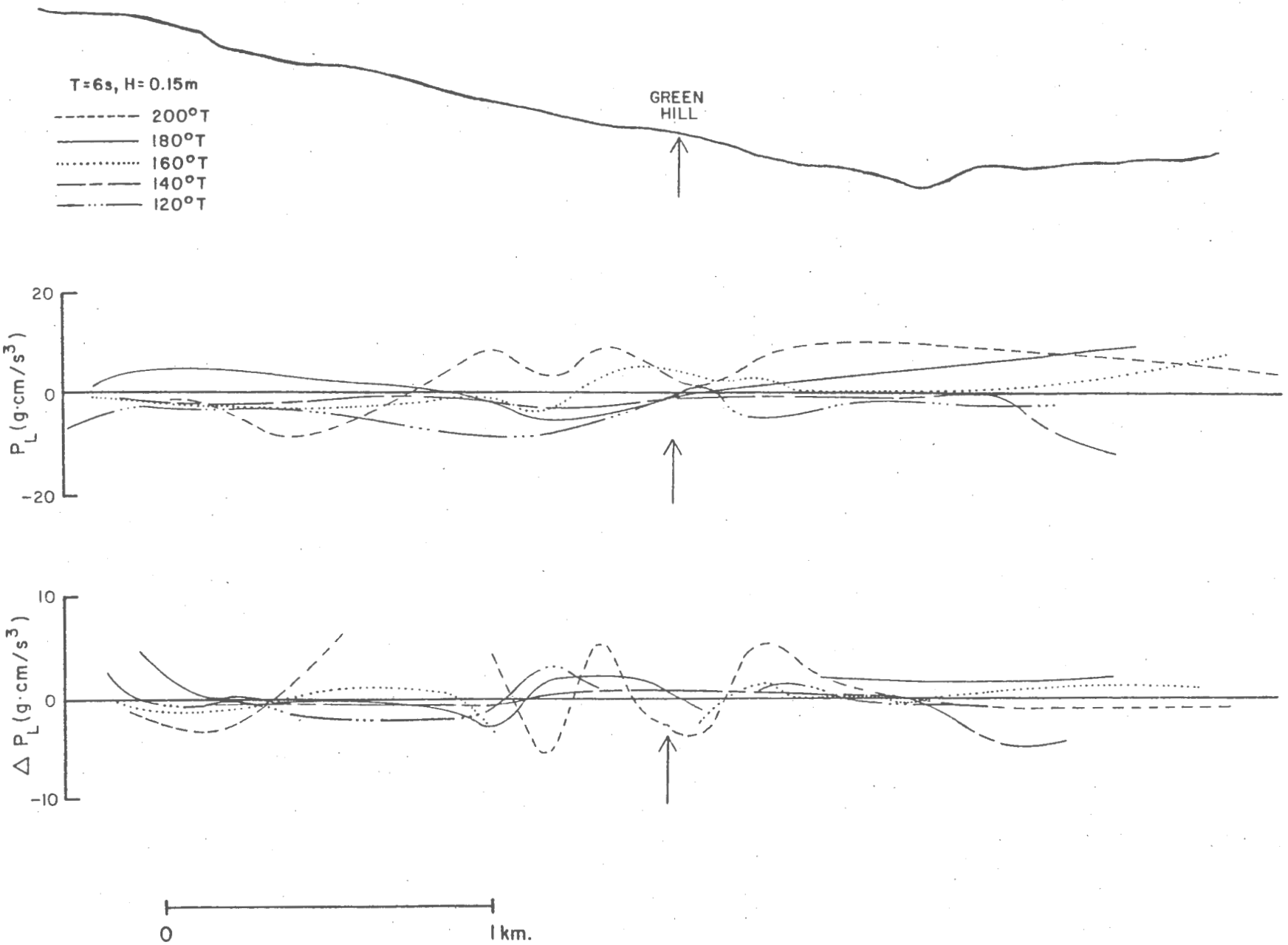
T=6s, H=0.15m
200°T
180°T
160°T
140°T
120°T
GREEN HILL
20
0
-20
P_L (g·cm/s^3)
10
0
-10
ΔP_L (g·cm/s^3)
0
1 km.